YAKUGAKU ZASSHI 127(3) 463—468 (2007) © 2007 The Pharmaceutical Society of Japan

—Reviews—

メチル水銀に対する感受性決定因子としてのユビキチン・プロテアソームシステム

黄　基旭

A Ubiquitin-proteasome System as a Factor that Determine the Sensitivity to Methylmercury

Gi-Wook HWANG

Laboratory of Molecular and Biochemical Toxicology, Graduate School of Pharmaceutical Sciences, Tohoku University, Aramaki, Aoba-ku, Sendai 980–8578, Japan

(Received November 27, 2006)

To elucidate the mechanism of toxicity of methylmercury (MeHg), we searched for factors that determine the sensitivity of yeast cells to MeHg and found that overexpression of Cdc34 or Rad23, both proteins related to the ubiquitin-proteasome (UP) system, induces resistance to MeHg toxicity. The acquisition of resistance to MeHg in Cdc34-overexpressing yeast cells requires the ubiquitin-conjugating activity of Cdc34 and the proteolytic activity of proteasomes. Therefore, it seems likely that certain as-yet-unidentified proteins that increase MeHg toxicity might exist in cells and that the toxicity of MeHg might be reduced by the enhanced degradation of such proteins through the UP system when Cdc34 is overexpressed. Unlike Cdc34, Rad23 suppresses the degradation of ubiquitinated proteins by proteasomes. This activity of Rad23 might be involved in the acquisition of resistance to MeHg toxicity when Rad23 is overexpressed. Overexpression of Rad23 might induce resistance to MeHg by suppressing the degradation of proteins that reduce the MeHg toxicity. Moreover, when we overexpressed Cdc34 in normal and Rad23-defective yeasts, resistance to MeHg was enhanced to almost the same extent in both lines of yeast cells. Thus it is possible that the binding of Rad23 to ubiquitinated proteins might be regulated by a mechanism that involves the recognition of substrate proteins and that the functions of Rad23 might not affect the protein-degradation system in which Cdc34 is involved. Many proteins that reduce or enhance MeHg toxicity and are ubiquitinated might exist in cells. The UP system and related proteins might determine the extent of MeHg toxicity by regulating the cellular concentrations of these various proteins.

Key words——methylmercury; toxicity; ubiquitin; proteasome; Cdc34; Rad23

1. はじめに

メチル水銀は主に中枢神経毒性を示す環境汚染物質であり，水俣病の原因物質としてもよく知られている．ヒトでのメチル水銀中毒はこれまでに水俣以外にも多くの国・地域で認められている．メチル水銀は食物連鎖によって魚類中に濃縮されるが，近年，妊娠中の女性が魚類を多く摂取することによって，未発達な胎児の脳にメチル水銀が影響を与える可能性が指摘され，世界的な社会問題ともなっている．しかし，メチル水銀による毒性発現機構及びそれに対する生体の防御機構はいまだほとんど解明されていない．

東北大学大学院薬学研究科生体防御薬学分野（〒980–8578 仙台市青葉区荒巻字青葉 6–3）
e-mail: gwhwang@mail.pharm.tohoku.ac.jp
本総説は，日本薬学会第 126 年会シンポジウム S16 で発表したものを中心に記述したものである．

これまでにわれわれは，メチル水銀毒性に対する防御機構を明らかにするために，真核単細胞生物であり，遺伝子産物の多くがヒトなどの哺乳動物と機能的に共通している出芽酵母（*Saccharomyces cerevisiae*）を用いてメチル水銀耐性獲得に係わる遺伝子の検索を行い，Bop3,[1] Cdc34,[2] GFAT[3] 及び Rad23[4] などを同定することに成功している．その中で，Cdc34 はユビキチン・プロテアソーム（UP）システムに係わるユビキチン転移酵素の一種であり，Rad23 も UP システム関連因子として知られている．UP システムは真核生物に広く保存されている蛋白質分解経路で，ユビキチン活性化酵素（E1），ユビキチン転移酵素（E2）及びユビキチンリガーゼ（E3）という 3 つの酵素の連続した働きによって細胞内で蛋白質にユビキチンを連結する．そして，ここでユビキチン化された蛋白質は，最終的にプロテアソームによって認識されて分解される

(Fig. 1).[5] 本稿では，選択的な蛋白質の分解経路であるUPシステムがメチル水銀毒性の発現機構において果たす役割について，筆者らの研究成果を中心に概説する．

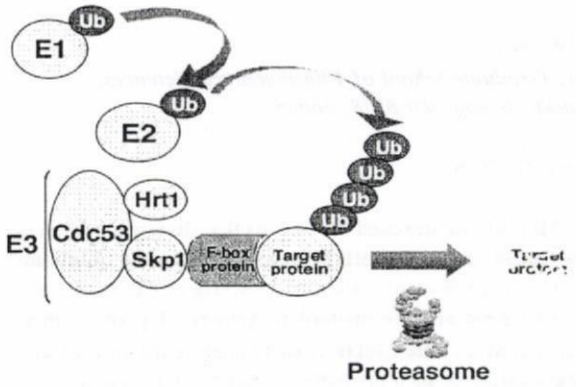

Fig. 1. Model for the SCF Complex-mediated Proteasomal Degradation

Proteins are targeted for degradation by the proteasome through the covalent attachment of ubiquitin (Ub) moieties. Ub activated by the ubiquitin-activating enzyme (E1) is transferred from E1 *via* ubiquitin-conjugating enzyme (E2) to the target protein. This final step is catalysed by ubiquitin ligase (E3). Multi-ubiquitinated proteins are degraded by the proteasome. Specific target recognition is the function of SCF complex, an E3. The complex is composed of a common core (Cdc53, Hrt1 and Skp1) and an F-box protein.

2. UPシステムを介した蛋白質分解の亢進によるメチル水銀の毒性軽減

Cdc34の構造中でメチル水銀耐性獲得に必要な機能ドメインを検索するために，E2活性に関与することが報告されている数ヵ所のドメインに変異を有するCdc34[6,7]をそれぞれ高発現する酵母を作製したところ，これらの酵母においてはメチル水銀に対する耐性は認められなかった（Fig. 2b）.[8] また，正常なCdc34を高発現させた酵母では総ユビキチン化蛋白質量の増加が認められたが，変異Cdc34を高発現させた酵母ではこのような現象も認められなかった（Fig. 2c）.[8] これらの結果は，Cdc34高発現によるメチル水銀耐性にCdc34が示すユビキチン転移活性が必須であることを示している．

Cdc34を介する蛋白質のユビキチン化には，E1であるUba1及びE3複合体の1つであるSCF（Skp1, Cdc53/cullin, F-box protein）が関与し，このE3複合体は4つのsubunit（Cdc53, Skp1, Hrt1, F-box protein）からなることが知られている（Fig. 1）.[9] しかし，この酵素群の各構成因子を高発現させてもE1高発現酵母でわずかなメチル水銀耐性が認められたものの，Cdc34高発現時に認められたよ

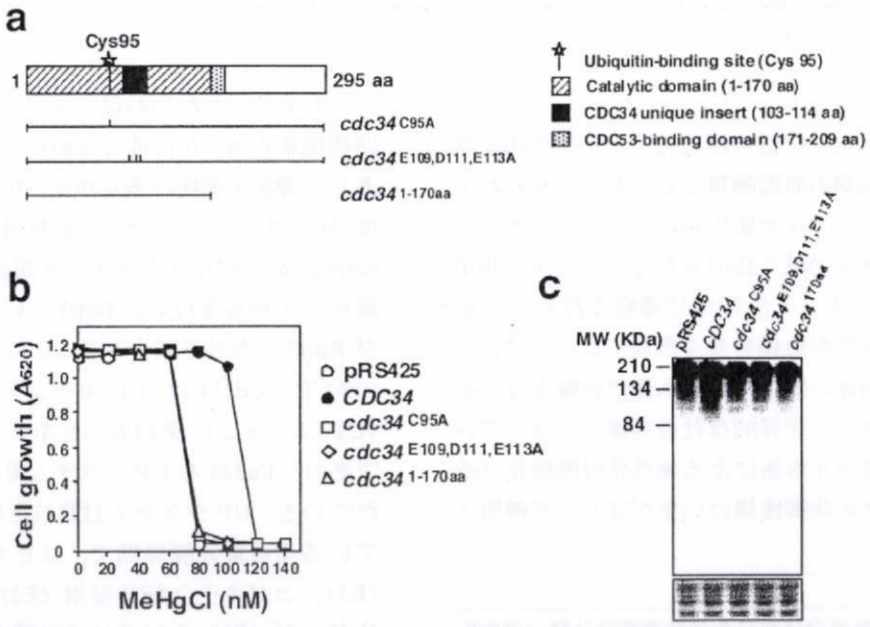

Fig. 2. Effects of the Overexpression of Cdc34 on the Sensitivity of Yeast Cells to Methylmercury

a: Structural domains of Cdc34 and construction of mutant proteins. b: Yeast strains carrying pRS425 (control), pRS425-*CDC34*, pRS425-*cdc34*^{C95A}, pRS425-*cdc34*$^{E109, D111, E113A}$ or pRS425-*cdc34*$^{1-170aa}$ were grown in SD (-leucine) medium in the presence of various concentrations of methylmercury. c: Lysates of each strain of yeast cells, cultured in control medium, were subjected to immunoblotting analysis with multiubiquitin-specific antibody. Staining with coomassie blue (lower panel) is shown as an indication of the amount of total protein loaded.

うな顕著な耐性は認められなかった．また，これら酵母の総ユビキチン化蛋白質量も正常酵母と同程度であった.[8]

一方，E2 は遺伝子ファミリーを形成しており，出芽酵母ではメチル水銀耐性因子として見出した Cdc34 以外にも，12 個の E2 分子種が同定されている.[10] そこで，これらのうちのいくつかの E2 の分子種を高発現する酵母を作製したところ，Cdc34 を高発現させた酵母よりもその程度は劣るものの，Ubc4, 5 又は 7 を高発現させた酵母もメチル水銀耐性が示し，これら酵母内のユビキチン化蛋白質量も正常酵母に比べて高値を示した.[8] ここで認められた耐性度の差は，恐らく各 E2 分子種の基質特異性の違いによるものと考えられる．以上の結果から，E2 はユビキチン化反応の律速酵素であり，本酵素群の高発現は細胞内における蛋白質のユビキチン化を促進させることによってメチル水銀毒性に対して防御的に作用するものと考えられる．

ユビキチン化された標的蛋白質は最終的にプロテアソームに認識されて速やかに分解される．Cdc34 高発現によるメチル水銀耐性はプロテアソーム阻害剤存在下では認められず（Fig. 3），また，遺伝子変異によって低プロテアソーム活性を示す酵母が対照酵母に比べて高いメチル水銀感受性を示すことも確認されたことから，Cdc34 高発現によるメチル水銀耐性にはプロテアソームによるユビキチン化蛋白質の分解が必須であると考えられる．

以上の結果から，細胞内にはメチル水銀毒性の増強に関与し，かつ，UP システムによって分解される蛋白質が存在し，Cdc34 はこの蛋白質のプロテアソームでの分解を亢進させることによってメチル水銀毒性に対して防御的に作用するものと考えられる.[9]

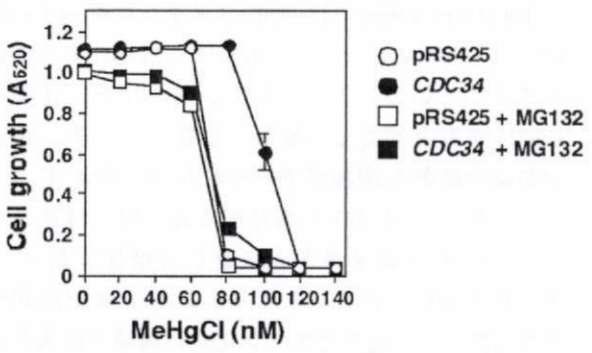

Fig. 3. Effects of a Proteasome Inhibitor on the Cdc34-mediated Resistance of Yeast Cells to Methylmercury

Yeast *erg6* cells that harbored pRS425 (control) or pRS425-*CDC34* were grown in SD (-uracil) liquid medium, with or without the proteasome inhibitor MG132 (50 μM), which had been dissolved in DMSO, and methylmercury at the indicated concentration.

一方，ヒトなどの高等動物においても多くの E2 分子種が存在することが知られている．ヒトの Cdc34 を高発現させた HEK293 細胞もメチル水銀に対して耐性を示すことから，ヒトにおいても Cdc34 が関与する UP システムがメチル水銀の毒性軽減機構として重要な役割を果たしている可能性が考えられる．したがって，メチル水銀毒性を増強させる蛋白質をヒト細胞中で同定することによって，ヒトにおけるメチル水銀の細胞内標的分子が明らかになるものと期待される．

3. メチル水銀の毒性軽減に係わる F-box 蛋白質の検索

SCF 複合体（E3）を構成する因子の中には，分解される基質蛋白質と直接結合する F-box 蛋白質が存在し，酵母では 17 種類が知られている.[11] この F-box 蛋白質を酵母に高発現させると，ユビキチン化される標的蛋白質と F-box 蛋白質を介した SCF 複合体との結合割合が増加し，標的蛋白質のユビキチン化とそれに続くプロテアソームでの分解が促進されると考えられる．したがって，メチル水銀毒性を増強させる蛋白質の分解に関与する F-box 蛋白質が高発現すると，その酵母はメチル水銀に対して耐性を示すと予想される．そこで，17 種の F-box 蛋白質をそれぞれ高発現する酵母を作製したところ，Hrt3 又は Ylr224w の高発現酵母が対照酵母に比べて強いメチル水銀耐性を示した.[12] F-box ドメインを欠失させた両 F-box 蛋白質の変異体を高発現させた酵母はメチル水銀耐性を示さず，また，プロテアソーム阻害剤の存在下では，Hrt3 又は Ylr224w の高発現酵母が示すメチル水銀耐性が認められないことから（Figs. 4 (a), (b)），[12] Hrt3 及び Ylr224w 高発現による酵母のメチル水銀耐性獲得には F-box ドメインを介した SCF 複合体の形成とユビキチン化された蛋白質のプロテアソームでの分解が必要であると考えられる．

以上のことから，Cdc34 又は F-box 蛋白質が高発現すると，F-box 蛋白質（Hrt3 又は Ylr224w）が認識する蛋白質のユビキチン化の亢進によってそれ

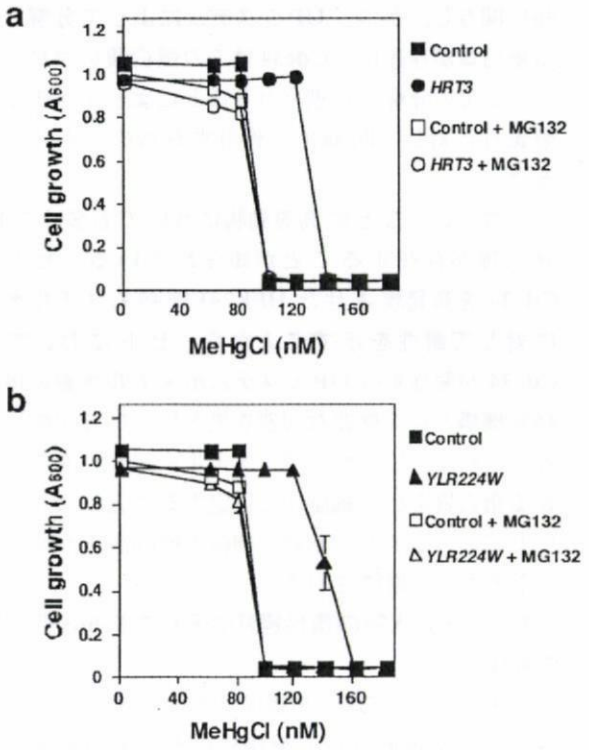

Fig. 4. Effects of a Proteasome Inhibitor on the Hrt3- and Ylr224w-mediated Resistance of Yeast Cells to Methylmercury

Yeast *erg6Δ* cells that harbored pKT10 or pKT10-*HRT3* (a) or pKT10 or pKT10-*YLR224W* (b) were grown in SD (-uracil) liquid medium, with or without the proteasome inhibitor MG132 (50 μM), which had been dissolved in DMSO, and methylmercury at the indicated concentration.

ら蛋白質のプロテアソームでの分解が促進され，その結果としてメチル水銀毒性が軽減されると考えられる．両 F-box 蛋白質の基質となる蛋白質は同定されていないが，両 F-box 蛋白質の基質蛋白質の中にメチル水銀毒性の増強に係わる蛋白質が含まれる可能性が高い．最近，われわれは両 F-box 蛋白質と特異的に結合し，かつ，メチル水銀の毒性増強に係わる蛋白質の同定に成功している．今後，これらの蛋白質がメチル水銀毒性の発現に果たす役割を検討することで，まだ不明な点が多いメチル水銀毒性発現機構の解明に重要な手掛かりが得られるものと期待される．

4. UP システムを介した蛋白質分解の抑制によるメチル水銀の毒性軽減

われわれは，高発現によって酵母にメチル水銀耐性を与える Cdc34 以外の UP システム関連因子として Rad23 を見出した．[4] Rad23 は UP システムによる蛋白質分解の促進及び抑制という相反する 2 つの機能によって UP システムによる蛋白質分解を調節していると考えられている．[13] Rad23 が示す蛋白質分解抑制作用は，Rad23 が有する 2 つの ubiquitin-associated（UBA）ドメインによるものであり，このドメインを介して Rad23 はユビキチン化蛋白質のユビキチン部分と結合し，それ以上ユビキチン鎖が伸長するのを阻害することによってその蛋白質の分解を抑制する．[14] 一方，Rad23 はユビキチン化蛋白質をプロテアソームに運搬する機能を有しており，これによって蛋白質の分解を促進させる．[15] この機能に必要な Rad23 中の領域は N 末端に存在する ubiquitin-like（UbL）ドメインであり，このドメインはユビキチンと相同性が高く，Rad23 はこのドメインを介してプロテアソームと結合することによってユビキチン化蛋白質の分解を亢進する役割を果たすと考えられている．[16]

Rad23 が有する 2 つの機能とメチル水銀毒性との関係を明らかにするために，Rad23 の UbL 及び 2 つの UBA ドメインをそれぞれ欠失させた truncation mutants を作製したところ，UbL ドメインを欠失した Rad23 を高発現させた酵母（ΔUbL）は，正常な Rad23 を高発現させた酵母よりも強いメチル水銀耐性を示し，両 UBA ドメインを欠失させた Rad23 を高発現させた酵母（ΔUBA1＋ΔUBA2）はメチル水銀耐性をほとんど示さなかった（Fig. 5(b)）．[4] すなわち，Rad23 の UbL ドメインはメチル水銀毒性を増強させる作用を有し，逆に UBA ドメインはメチル水銀耐性に係わっていると考えられる．正常な Rad23 を高発現させた酵母はメチル水銀耐性を示すことから，これらの結果は，少なくとも Rad23 高発現時には UbL ドメインに由来する機能よりも UBA ドメインに由来する機能の方が優位に作用していることを示している．また，正常な Rad23 を高発現させた酵母では総ユビキチン化蛋白質量の顕著な増加が認められたが，UbL ドメインを欠失した Rad23 を高発現させた際には総ユビキチン化蛋白質量がさらに著しく増加した．[4] 一方，両 UBA ドメインを欠失した Rad23 を高発現させた際には，総ユビキチン化蛋白質量の顕著な減少が認められた．[4] この結果は，Rad23 が有する UbL ドメインはユビキチン化蛋白質の細胞内濃度を減少させ，UBA ドメインは逆に増加させる機能を担っていることを示している．

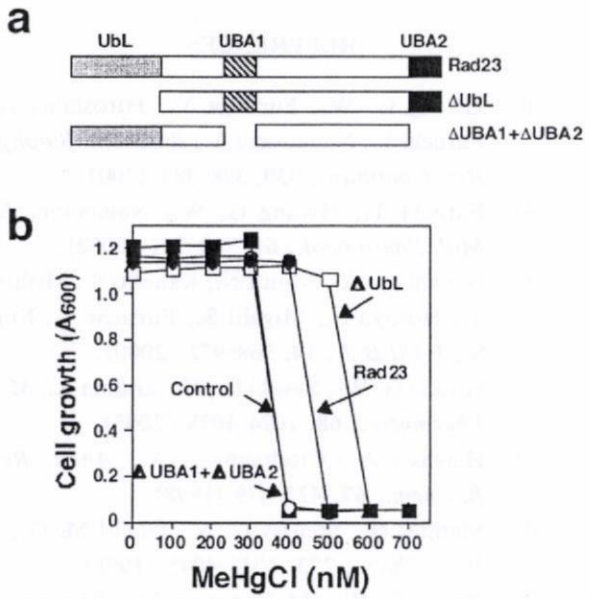

Fig. 5. Effects of Overexpression of Mutant Forms of Rad23 on the Sensitivity of Yeast Cells to Methylmercury

a: Schematic representation of the structural domains of Rad23 and the mutant proteins generated in this study. Rad23 contains a ubiquitin-like (UbL) domain and two ubiquitin-associated (UBA) domains. b: Yeast cells that overexpressed FLAG-Rad23 or mutant derivatives were cultured in SD (-uracil) liquid medium that contained methylmercury at the indicated concentrations.

以上の結果から，Rad23 が有する 2 つの機能のうち，UBA ドメインを介したユビキチン化蛋白質の分解抑制作用はメチル水銀毒性を軽減し，UbL ドメインを介したユビキチン化蛋白質の分解促進作用はメチル水銀毒性を増強するが，Rad23 高発現酵母中では，ユビキチン化蛋白質の分解抑制作用の方が分解促進作用を凌いでいるために，Rad23 高発現酵母はメチル水銀に対して耐性を示すと考えられる．したがって，細胞内にはメチル水銀毒性の軽減に関与し，かつ，UP システムによって分解される蛋白質が存在し，Rad23 はこの蛋白質の分解を抑制することによってメチル水銀毒性に対して防御的に作用していると考えられる．

5. メチル水銀毒性発現における Cdc34 と Rad23 との係わり

Rad23 は，Cdc34 とは逆に，メチル水銀毒性を軽減する蛋白質の分解を抑制することによってメチル水銀毒性を軽減する可能性が示された．しかし，Cdc34 は蛋白質のユビキチン化に関与し，Rad23 はユビキチン化蛋白質のユビキチン鎖と結合することから，Cdc34 と Rad23 がメチル水銀毒性に間接的に係わる同一の蛋白質を基質として認識する可能性も否定できない．そこで，正常酵母と Rad23 欠損

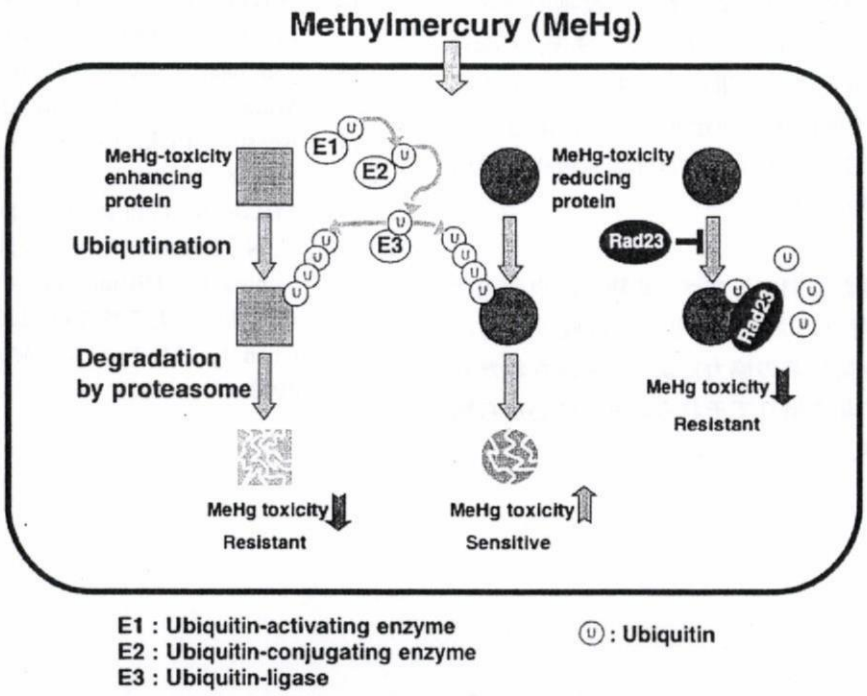

Fig. 6. Regulation of Methylmerury Toxicity by Ubiquitin-proteasome System

酵母にそれぞれ Cdc34 を高発現させたところ，両酵母のメチル水銀に対する耐性度はほぼ同程度に上昇した．このことから Rad23 とユビキチン化蛋白質のユビキチン鎖との結合は何らかの厳密な基質蛋白質認識機構によって調節されており，Cdc34 が E2 として関与する蛋白質分解システムに Rad23 の機能はほとんど影響を与えないと考えられる．細胞内にはメチル水銀毒性を軽減又は増強し，かつ，ユビキチン化を受ける複数の蛋白質が存在し，UP システム及び関連蛋白質はそれら蛋白質の細胞内濃度を複雑に調節することによってメチル水銀毒性の発現程度を規定していると考えられる（Fig. 6）．

6. おわりに

近年，様々な神経変性疾患の発症に UP システムが係わっていることが多く報告されており，UP システムの異常は脳機能に大きな障害をもたらすものと考えられる．一方，メチル水銀も主に中枢神経障害を引き起こすことから，UP システムとメチル水銀毒性との関係も注目すべき事実と考えられる．これまでに筆者らが得た知見は，メチル水銀に対する感受性決定機構として UP システムが重要な役割を果たしている可能性を強く示唆するものである．これらの知見はメチル水銀細胞毒性の発現機構及びそれに対する防御機構の解明に有用な手掛かりを与えるだけでなく，UP システムの新しい役割の解明にも大きく貢献し得るものと思われる．今後，Cdc34 及び Rad23 の基質となる蛋白質の中からメチル水銀毒性に係わる蛋白質を同定することによって，UP システムによるメチル水銀毒性調節機構が解明されるものと期待される．

謝辞　本総説に関するすべての研究は東北大学大学院薬学研究科において永沼　章教授の指導の下，多くの大学院生等の協力によって実施されたものであり，この場を借りてそれらの方々に心から感謝申し上げます．

REFERENCES

1) Hwang G. W., Furuoya Y., Hiroshima A., Furuchi T., Naganuma A., *Biochem. Biophys. Res. Commun.*, **330**, 378–385 (2005).
2) Furuchi T., Hwang G. W., Naganuma A., *Mol. Pharmacol.*, **61**, 738–741 (2002).
3) Naganuma A., Miura N., Kaneko S., Mishina T., Hosoya S., Miyairi S., Furuchi T., Kuge S., *FASEB J.*, **14**, 968–972 (2000).
4) Hwang G. W., Sasaki D., Naganuma A., *Mol. Pharmacol.*, **68**, 1074–1078 (2005).
5) Hershko A., Ciechanover, A., *Annu. Rev. Biochem.*, **67**, 425–479 (1998).
6) Mathias N., Steussy C. N., Goebl M. G., *J. Biol. Chem.*, **273**, 4040–4045 (1998).
7) Pitluk Z. W., McDonough M., Sangan P., Gonda D. K., *Mol. Cell. Biol.*, **15**, 1210–1219 (1995).
8) Hwang G. W., Furuchi T., Naganuma A., *FASEB J.*, **16**, 709–711 (2002).
9) Deshaies R. J., *Annu. Rev. Cell Dev. Biol.*, **15**, 435–467 (1999).
10) VanDemark A. P., Hill C. P., *Curr. Opin. Struct. Biol.*, **12**, 822–830 (2002).
11) Craig K. L., Tyers M., *Prog. Biophys. Mol. Biol.*, **72**, 299–328 (1999).
12) Hwang G. W., Ishida Y., Naganuma A., *FEBS Lett.*, **580**, 6813–6818 (2006).
13) van Laar T., van der Eb A. J., Terleth C., *Mutat. Res.*, **499**, 53–61 (2002).
14) Raasi S., Pickart C. M., *J. Biol. Chem.*, **278**, 8951–8959 (2003).
15) Elsasser S., Gali R. R., Schwickart M., Larsen C. N., Leggett D. S., Muller B., Feng M. T., Tubing F., Dittmar G. A., Finley D., *Nat. Cell. Biol.*, **4**, 725–730 (2002).
16) Chen L., Madura K., *Mol. Cell. Biol.*, **22**, 4902–4913 (2002).

JOURNAL OF CELLULAR PHYSIOLOGY 210:378–384 (2007)

Cisplatin Upregulates *Saccharomyces cerevisiae* Genes Involved in Iron Homeostasis Through Activation of the Iron Insufficiency-Responsive Transcription Factor Aft1

AKIKO KIMURA,[1] KAZUAKI OHASHI,[1,2] AND AKIRA NAGANUMA[1,3]*

[1]*Laboratory of Molecular and Biochemical Toxicology, Graduate School of Pharmaceutical Sciences, Tohoku University, Sendai, Japan*

[2]*Laboratory of Biochemistry and Molecular Biology, Graduate School of Pharmaceutical Sciences, Osaka University, Osaka, Japan*

[3]*Tohoku University 21st Century COE Program "Comprehensive Research and Education Center for Planning of Drug Development and Clinical Evaluation" Sendai, Japan*

The response of *Saccharomyces cerevisiae* to cisplatin was investigated by examining variations in gene expression using cDNA microarrays and confirming the results by reverse transcription polymerase chain reaction (RT-PCR). The mRNA levels of 14 proteins involved in iron homeostasis were shown to be increased by cisplatin. Interestingly, the expression of all 14 genes is known to be regulated by Aft1, a transcription factor activated in response to iron insufficiency. The promoter of one of these genes, *FET3*, has been relatively well studied, so we performed a reporter assay using the *FET3* promoter and showed that an Aft1 binding site in the promoter region is indispensable for induction of transcription by cisplatin. The active domain of Aft1 necessary for activation of the *FET3* promoter by cisplatin is identical to the one required for activation by bathophenanthroline sulfonate, an inhibitor of cellular iron uptake. Furthermore, we found that cisplatin inhibits the uptake of ^{55}Fe(II) into yeast cells. These findings suggest that cisplatin activates Aft1 through the inhibition of iron uptake into the cells, after which the expression of Aft1 target genes involved in iron uptake might be induced. J. Cell. Physiol. 210: 378–384, 2007. © 2006 Wiley-Liss, Inc.

Cisplatin is an anticancer drug that is effective against various malignant tumors, including those of the testis, ovary, prostate gland, and uterus (Einhorn and Williams, 1979). However, acquisition of resistance to cisplatin by tumor cells and the development of adverse effects are disadvantageous in its clinical usage. A number of mechanisms have been implicated in the acquisition of cisplatin resistance, including decreases in the amount of cisplatin taken up by cells (Kikuchi et al., 1990; Gately and Howell, 1993), augmented cellular excretion of cisplatin (Ishikawa and Ali-Osman, 1993; Mistry et al., 1993; Fujii et al., 1994; Aebi et al., 1996; Fink et al., 1997), enhancement of detoxification mechanisms due to concentration increases in glutathione and metallothioneins (Naganuma et al., 1987; Kelley et al., 1988; Godwin et al., 1992; Ikeda et al., 2001), and inhibition of apoptotic signals (Siddik, 2003). However, in many types of tumor cells, the development of resistance cannot be explained only by these mechanisms, indicating the possible presence of other unknown processes.

Recently, comprehensive genetic analyses have been carried out of various organisms to elucidate the mechanisms behind the acquisition of resistance. Studies of the cells of budding yeasts (Brown et al., 1993; Fox et al., 1994; Furuchi et al., 2001; Niedner et al., 2001; Schenk et al., 2001, 2003; Huang et al., 2005), *Dictyostelium discoideum* (Niedner et al., 2001), and mammals (Niedner et al., 2001; Ishida et al., 2002) identified several genes involved in cisplatin-resistance. However, few studies have examined the cellular response to cisplatin. Genetic examination of budding yeasts is easily conducted and there is a wealth of information regarding the function of each gene. Furthermore, the functions of many yeast genes are common to those of mammalian genes including those of humans. Thus, the findings obtained from yeast studies provide an insight into the functions of human proteins.

Using budding yeast as a model organism, we used cDNA microarray technology to investigate variations in gene expression following cisplatin treatment. We found that the mRNA levels of many proteins involved in the maintenance of iron homeostasis were increased by cisplatin. Furthermore, we demonstrated for the first time that cisplatin inhibits iron uptake into eukaryotic cells, leading to iron deficiency and the consequent activation of the transcription factor Aft1. Our findings suggest that target genes of Aft1 involved in the maintenance of iron homeostasis are augmented in response to cisplatin.

Abbreviations: YPAD, yeast extract–peptone–adenine–dextrose; SD, synthetic dextrose; PCR, polymerase chain reaction; RT-PCR, reverse transcription polymerase chain reaction; BPS, bathophenanthroline sulfonate, MUG, methyl umbelliferyl β-D galactopyranoside; WT, wild type.

Contract grant sponsor: Health and Labour Sciences Research Grants for Research on Risk of Chemical Substances from Ministry of Health, Labour and Welfare Japan; Contract grant number: H17-Risk of Chemical Substances-010.

*Correspondence to: Akira Naganuma, Laboratory of Molecular and Biochemical Toxicology, Graduate School of Pharmaceutical Sciences, Tohoku University, Aoba-ku, Sendai 980-8578, Japan. E-mail: naganuma@mail.pharm.tohoku.ac.jp

Received 5 June 2006; Accepted 25 July 2006

Published online in Wiley InterScience (www.interscience.wiley.com.), 9 November 2006.
DOI: 10.1002/jcp.20845

MATERIALS AND METHODS

Yeast strains and media

BY4742 (*MATα; his3Δ1; leu2Δ0; lys2Δ0; ura3Δ0*) and *aft1Δ* (*MATα; his3Δ1; leu2Δ0; lys2Δ0; ura3Δ0; YGL071W:kanMX4*) were obtained from Euroscarf (Frankfurt, Germany). Yeast cells were grown on yeast extract–peptone–adenine–dextrose (YPAD) medium (1% yeast extract, 2% peptone, 0.004% adenine, and 2% glucose) or on synthetic dextrose (SD) medium supplemented with amino acids. Transformation of yeast cells was performed by the lithium acetate method (Naganuma et al., 2000).

Construction of pMELb2-FET3-lacZ, pMELb2-FIT3-lacZ, pMELb2- LM2-lacZ, and pMELb2-Aft1 binding site–lacZ

The *FET3* and *FIT3* promoters were amplified by polymerase chain reaction (PCR) using yeast chromosomal DNA as a template and the following primers: *FET3* promoter-F and *FET3* promoter-R for *FET3*, and *FIT3* promoter-F and *FIT3* promoter-R for *FIT3* (Table 1). The PCR product was digested with *Hind*III and *Bam*HI, and the fragment was cloned into the *Bam*HI–*Hind*III sites of pMELb2, a *LacZ* expression vector. The mutant *FET3* promoter (LM2) (Yamaguchi-Iwai et al., 1996) was amplified by PCR using pMELb2 *FET3-lacZ* as a template and the primer pair LM2-F and LM2-R (Table 1). The PCR product was then self-ligated.

The Aft1 binding site was created by annealing the oligonucleotides Aft1 binding site-F, 5′-TCGACGAGCACCTGCAATGGGTGCACTTTTGAAG-3′, and Aft1 binding site-R, 5′-TCGACTTCAAAAGTGCACCCATTTGCAGGTGCTCG-3′. The annealed oligonucleotides were cloned into the *Xho*I sites of pMELb2.

Construction of pRS315-AFT1-GFP-GFP-HA. The *AFT1* gene containing 759-bp upstream from the transcriptional start site was amplified by PCR using yeast chromosomal DNA as a template and the primer pair AFT1-F and AFT1-R (Table 1). The PCR product was digested with *Sac*I and *Eco*RV, and the fragment was cloned into the *Sac*I–*Sma*I sites of pRS315-Met-GFP-GFP-HA (Isoyama et al., 2001).

Construction of yeast strains overexpressing mutant forms of Aft1p

The *AFT1* deletion mutants M1–M14 were constructed by creating pairs of *Kpn*I sites in the *AFT1* gene and self-ligating between the respective pairs of *Kpn*I sites. First, pRS315-*AFT1*-GFP-GFP-HA was digested with *Sac*I and *Apa*I, and the fragment cloned into the *Sac*I–*Apa*I site of the pGEM-T easy vector (Promega, Madison, WI). PCR mutagenesis was performed on pGEM-T easy-*AFT1*-GFP-GFP-HA using corresponding sets of primers (Table 1). The amplification added a *Kpn*I site to both ends of the PCR products so, after amplification, the PCR products were cleaved with *Kpn*I and self-ligated, resulting in the removal of the amino acids shown in Figure 5A. Each pGEM-T easy-*AFT1* deletion mutant (M1–M14) was digested with *Sac*I and *Apa*I and the fragment was ligated into pRS315. To create the deletion mutant M15, pRS315-*AFT1* was digested with *Hind*III and the fragment religated. Each deletion mutant (pRS315-*AFT1* mutants) was then introduced into *aft1Δ* cells.

Microarray

Yeast (5×10^6 cells/ml) was precultured in SD medium for 3 h at 30°C. Cells were then cultured in SD medium for 3 h with or without 100 μM cisplatin (Nippon Kayaku, Tokyo, Japan). The suspension was centrifuged at 2,200*g* for 5 min and the cells were collected. Total RNA was isolated using the hot acidic phenol method (Furuchi et al., 2002), after which poly $(A)^+$ mRNA was isolated from 250 μg total RNA using the Oligotex^{TM} –dt30^{mRNA} kit (JSR, Tokyo, Japan). Fluorescent-labeled cDNA was generated using an oligo dT primer with Fluorilink Cy3-dUTP or Fluorilink Cy5-dUTP and SuperScript^{TM} II RT (Invitrogen, Carlsbad, CA). Cy3- and Cy5-labeled cDNA probes were combined and hybridized to Yeast Chip ver2.0. (Hitachi Software Engineering, Kanagawa, Japan) in 5× SSC at 65°C for 14–16 h. After washing, the microarray slides were simultaneously scanned by a GenePix 4000B array scanner (Axon Instruments, Union City, CA). Array-Pro Analyzer 4.5 analysis software (LI-COR Biosciences, Lincoln, NE) was used to analyze the results.

RT-PCR

Total RNA was extracted using the hot acidic phenol method (Furuchi et al., 2002). cDNA was synthesized from 3 mg total RNA using 0.5 mM oligo dT primer, 50 U Molony Murine Leukemia Virus reverse transcriptase, and 10 U RNA nuclease inhibitor. Reverse transcription polymerase chain reaction (RT-PCR) was performed using SYBR *premix Ex Taq*^{TM} (TaKaRa, Shiga, Japan). Reverse transcribed mRNA was diluted 10-fold and 0.5 μl of the diluted solution was used as a template for PCR with specific primers (Table 1) to amplify the following genes: *ARN1, ARN2, ARN3, CCC2, CCP1, FIT1, FIT2, FIT3, FET3, FET4, FRE1, FRE2, FRE3, FTR1, HMX1, HSP30, TIS11, YHL035C,* and *YMR251W-R*. The amplified DNA was scanned by the iCycler iQ real-time PCR detection system (Bio-Rad, Philadelphia, PA). Each transcript was quantified relative to the Glyceraldehyde-3-phosphate dehydrogenase standard.

β-Galactosidase assay

β-Galactosidase reporter constructs were transformed into either BY4742 or *aft1Δ* cells. Yeast cells carrying a reporter plasmid at mid-logarithmic phase were cultured in SD medium with or without non-toxic concentration of cisplatin for 3 h. The culture was centrifuged at 2,200*g* for 5 min to remove the supernatant. Cells were resuspended in 25 μl Tris-Triton buffer (0.1 M Tris-HCl, pH 7.5; 0.05% Triton X-100). The suspensions were frozen, thawed, and incubated with 125 μl Z buffer (10 mM KCl, 60 mM Na_2HPO_4, 40 mM NaH_2PO_4, 1 mM $MgSO_4$) containing 0.5 mg/ml methyl umbelliferyl β-D galactopyranoside (MUG) at 30°C for 5 min. The absorbance of MUG at $^{EX}360$ nm $^{EM}450$ nm was measured. After adjusting cell density (OD_{600}) and reaction time (min), the value was taken as an index of β-galactosidase activity. The assay was repeated at least three times.

Iron uptake assay

Ferrous uptake was assayed as described by Dancis et al. (1990) with a few modifications. Yeast cells ($OD_{600} = 0.5$) were collected by centrifugation and resuspended in ice-cold assay buffer (5% glucose, 50 mM sodium citrate, pH 6.5) to $OD_{600} = 5$. Then 1 μM $^{55}FeCl_3$ (Perkin Elmer, Wellesley, MA, 74 MBq/ml) and 1 μM ascorbate were added with or without non-toxic concentration of cisplatin. The suspensions were incubated at 30°C for 1, 2, or 3 h, and filtered through a glass filter. The radioactivity retained on the filters was measured using imaging plates (Fuji Photo Film, Kanagawa, Japan) and a BAS-5000 imaging analyzer (Fuji Photo Film).

RESULTS

To examine the effect of cisplatin treatment on budding yeasts, we used DNA microarray technology to study the variation in gene expression after incubation with 100 μM cisplatin for 3 h. A more than twofold increase in the expression of 18 genes and a more than twofold decrease in the expression of 2 genes was detected (Table 2).

Variation in expression following cisplatin treatment was confirmed by RT-PCR analysis for all genes, with the exception of *FIT1, YPR123C, HSP30,* and *CCP1* (Table 2). Interestingly, among the 16 genes whose expression was increased by cisplatin, 14 were shown to be involved in the maintenance of iron homeostasis. Fit2 and Fit3 hold iron within the cell wall (Protchenko et al., 2001); Arn 1–3 are components of a siderophore transporter complex produced by microorganisms and iron (III) (Lesuisse et al., 1998; Heymann et al., 1999, 2000); Fre 1–3 are iron reducing enzymes (Georgatsou and Alexandraki, 1994; Martins et al., 1998); Fet 4 is a low-affinity iron transporter (Dix et al., 1994); Fet3 is a constituent factor of a high affinity iron transport

TABLE 1. Primer Sequences used in plasmid construction and creation of deletion mutants

Primer pair	Sequence (5′-3′)[a]	Amplification
AFT1-F	GATCGAGCTCTCTAGATACACAGGGCAAGGTCATTA	*AFT1*
AFT1-R	GATCGATATCGCCATCTTCTGGCTTCACAT	
ARN1-F	ACCCTCTATAGAATTGGTTCT	*ARN1*
ARN1-R	CGACATATTCGCCATCCTC	
ARN2-F	GGCTAACGTTGTTTCTTGT	*ARN2*
ARN2-R	CCTGTAATTCTTTCCATTCCA	
ARN3-F	GTAACCTCATTATACCTTGC	*ARN3*
ARN3-R	CCTATCTTTACTGCTTGTAAA	
CCC2-F	GAGAGGACTGGCCAACG	*CCC2*
CCC2-R	CGGCCTGTGATTCTATGTC	
CCP1-F	CGCTGACTATGTCAGAACA	*CCP1*
CCP1-R	CCTTGTTCCTCTAAAGTC	
FET3-F	GCAAGGTTTGGGTCTTGTTC	*FET3*
FET3-R	GATGCTTTTCAGTGGAATGAC	
FET3 promoter-F	GCAAGCTTTTTCCGGGTGCGAATCAG	*FET3*
FET3 promoter-R	GCGGATCCAAACATCTAGTTCTAATTTTTTGC	
FET4-F	GGTGGTTGATTATCGGTACA	*FET4*
FET4-R	CCCAATTATGTGCTTGCAAC	
FIT1-F	TCTAAATCCACGTCTGCAGT	*FIT1*
FIT1-R	CGGTAGTGGTTTGAACTCTTG	
FIT2-F	ACAGTTATGACTGCCGTCTCG	*FIT2*
FIT2-R	ACACTTGCTCCTTGGAATGCA	
FIT3-F	TTTTGTCTGGACTGGTGAAGG	*FIT3*
FIT3-R	CAGCACCCATCAAACCAGTA	
FIT3 promoter-F	GCAAGCTTCTCCATAAACATTTCCTTTGTC	*FIT3*
FIT3 promoter-R	GCGGATCCAAACATTTTAGGGATTATTGTTATTAG	
FRE1-F	GCTATTTATCCGCACTTTGTC	*FRE1*
FRE1-R	CTTTCTTCTTCTAGTTCAACG	
FRE2-F	GGCTTATAAGCCGGAGTTG	*FRE2*
FRE2-R	GCATTGATACTCTTCAAAGTA	
FRE3-F	CGTACTCGAGGCTTACAAG	*FRE3*
FRE3-R	CTTCAAAGTATTCGATTGCC	
FTR1-F	GTGCTTCGAAATCCTCGCTG	*FTR1*
FTR1-R	CTCTTTTGCTCTTCCGTCAAC	
HMX1-F	CCCACTGAAGAAACACGCTT	*HMX1*
HMX1-R	GTGCTCTTCTAGTAGCAGAATCC	
HSP30-F	GGTGTGATATGCCAACGTC	*HSP30*
HSP30-R	CAGGTTCGGGTTCGTGG	
LM2-F	GGCCCATCTTCAAAAGTGCAGGGATTTGCAGGTGCTC	LM2
LM2-R	GAGCACCTGCAAATCCCTGCACTTTTGAAGATGGGCC	
TIS11-F	GCAACAGTTGTCTCAACA	*TIS11*
TIS11-R	GGTCATTCTCTGCAAAGC	
YHL035C-F	GAGGAACGCTTTAACAGCA	*YHL035C*
YHL035C-R	CATCTTACTTGATTGCTTGG	
YMR251W-F	CAGAGTTCAACTCTTGGGTG	*YMR251W*
YMR251W-R	GTGGGGTGATCCCAATC	
YPR123C-F	CCATATCCATCCCTGAAGA	*YPR123C*
YPR123C-R	CATTTGTTGGAAGAATCGAAT	
M1-F	GC**GGTACC**GAACATGCGTCACCGATTAATTCATCTGACAGC	M1
M1-R	CG**GGTACC**CATTGTCGTAGATTTTTCTGTTATTTTTTTGTT	
M2-F	GC**GGTACC**GAGGGTCGTGCAAGTGCAAGTGG	M2
M2-R	CG**GGTACC**TATGTCAGCCGGATTGAAGCCTTCC	
M3-F	GC**GGTACC**AACAATTTGATTCATCTGGATCCAGTACCCAAC	M3
M3-R	CG**GGTACC**ATTATGGTTGACTACATATTCACTAGCACTTTTGGG	
M4-F	GC**GGTACC**TTTGAAGATAAGTCCGATATTAAGCCTTGG	M4
M4-R	CG**GGTACC**TTGATTCAGCTTTTCCACATGATGAATATGC	
M5-F	GC**GGTACC**AAGCCCAAAGAAAAAAAGATGTGTATCGAGG	M5
M5-R	CG**GGTACC**TTTTCTTTTCCTTCTCGCGTTCCTTCCCC	
M6-F	GC**GGTACC**TGTGTATCGAGGTTTAATAACTGTCCG	M6
M6-R	CG**GGTACC**TATGGAGGATGTTTGATCGGGCG	
M7-F	GC**GGTACC**TCTAAAAGGCCATGCTTACCCTCTG	M7
M7-R	CG**GGTACC**TTTCTTGATTGCATCTACGTCATTATCC	
M8-F	GC**GGTACC**TGCTTACCCTCTGTAAATAACACCGG	M8
M8-R	CG**GGTACC**TGCATTCGATGAATCAAGGGATATGGACG	
M9-F	GC**GGTACC**AGGAAACCGAAAAGCCAGTGTAAGAATAAAG	M9
M9-R	CG**GGTACC**TGGCCTTTTAGATGCATTCGATGAATCAAG	
M10-F	GC**GGTACC**CAGTGTAAGAATAAAGACACACTCTTAAAAAG	M10
M10-R	CG**GGTACC**TACGTTATTGGTATTGATACTACCGGTG	
M11-F	GC**GGTACC**CCGGCATCCGATTTCAAGCTAAAC	M11
M11-R	CG**GGTACC**GCTTTTCGGTTTCCTTACGTTATTGG	
M12-F	GC**GGTACC**CAAGAAGCTTTAGTTGGCAGCTCTTC	M12
M12-R	CG**GGTACC**CAGTGGCAAGATTTCATTCAAATTGAAAGG	

[a]Bold letters indicate *Kpn*I sites.

system and an oxidizing enzyme of iron (Askwith et al., 1994); Ftr1 is an iron permease (Stearman et al., 1996); Hmx 1 is a factor resembling heme-oxygenase (Auclair et al., 2003), a copper transporter that transfers iron to Fet3 (Fu et al., 1995); and Tis11 is a factor that breaks down the mRNA of an iron-containing enzyme when the cell is deficient in iron (Puig et al., 2005) (Table 2).

TABLE 2. Yeast genes whose expression levels were changed by treatment with cisplatin

Gene	ID	Fold-increase		Function
		Microarray	RT-PCR	
FIT2[a]	*YOR382W*	49.3	19.1	Cell wall protein involved in iron uptake
FIT3[a]	*YOR383C*	30.6	10.9	Cell wall protein involved in iron uptake
ARN2[a]	*YHL047C*	9.2	7.9	Siderophore transporter
FIT1[a]	*YDR534C*	8.6	1.1	Cell wall protein involved in iron uptake
ARN3[a]	*YEL065W*	5.8	3.8	Siderophore transporter
FRE2[a]	*YKL220C*	4.8	4.5	Ferric and cupric reductase
HMX1[a]	*YLR205C*	4.7	3.0	Heme-binding protein
ARN1[a]	*YHL040C*	4.3	2.9	Siderophore transporter
FRE1[a]	*YLR214W*	4.2	3.1	Ferric and cupric reductase
FRE3[a]	*YOR381W*	3.2	1.9	Ferric reductase
FET3[a]	*YMR058W*	3.0	2.5	High-affinity Fe(II) transporter
FTR1[a]	*YER145C*	2.9	2.2	Iron permease
FET4[a]	*YMR319C*	2.2	2.5	Low-affinity Fe(II) transporter
CCC2[a]	*YDR270W*	2.5	2.3	Copper transporter
TIS11[a]	*YLR136C*	6.8	19.5	Protein of the CCCH zinc finger family
VMR1	*YHL035C*	2.0	2.0	Unknown
	YMR251W	4.5	3.9	Unknown
	YPR123C	2.3	1.0	Unknown
HSP30	*YCR021C*	0.3	0.8	Heat shock protein
CCP1	*YKR066C*	0.5	ND	Cytochrome-c peroxidase

ND, not detected.
[a]Genes whose expression is known to be regulated by Aft1.

It is known that the expression of many genes involved in cellular uptake of iron are regulated by the transcription factor Aft1 (Yamaguchi-Iwai et al., 1996). In the present study, we found that all 14 genes involved in maintaining iron homeostasis whose expression was augmented by cisplatin were regulated by Aft1 (Table 2). It is therefore possible that the augmentation of expression by cisplatin is also regulated by Aft1. To investigate this, we conducted a β-galactosidase reporter assay using plasmids expressing the *LacZ* gene under the control of *FIT3* and *FET3* promoters with Aft1 binding sites. The results showed that *FIT3* and *FET3* promoter activities increased in a dose-dependent manner with increasing concentrations of cisplatin (Fig. 1).

Next, we examined the effects of Aft1 deficiency on cisplatin activation of the *FET3* promoter (Yamaguchi-Iwai et al., 1996). Cisplatin had a negligible effect on *FET3* promoter activation in an Aft1-deficient, compared with a wild-type, yeast strain (Fig. 2A). Similarly, when the Aft1 binding site (TGCACCCA) was used in place of the *FET3* promoter (245–252 bp upstream from the *FET3* transcription start site), cisplatin effected an increase in β-galactosidase activity of the wild-type strain, but had no effect on reporter gene activity in the Aft1-deficient yeast (Fig. 2B). A previous study by Yamaguchi-Iwai et al. (1996) showed that Aft1 was unable to bind a mutant *FET3* promoter, LM2, with a CCC → GGG mutation in its Aft1 binding site. We therefore examined the effect of cisplatin by carrying out a reporter gene assay in yeast expressing *LacZ* under the control of the LM2 promoter and showed that cisplatin did not affect promoter activity (Fig. 2C). From the above findings, we conclude that cisplatin augments the expression of genes involved in maintaining iron homeostasis, such as *FET3*, by promoting Aft1 binding to a site present within the promoter region of Aft1 target genes.

Aft1 is usually present within the cytoplasm, but is translocated to the nucleus during periods of cellular iron deficiency, where it binds to the promoter of its target genes and accelerates their transcription (Yamaguchi-Iwai et al., 1995, 2002). Bathophenanthroline sulfonate (BPS) is a chelating agent of bivalent iron that is unable to penetrate the cell membrane and is capable of chelating iron in cell growth medium. As such, it is used as an inhibitor of iron uptake into cells (Alcain et al., 1994). We applied BPS to the reporter gene assay in wild-type and Aft1-deficient yeasts examined in Figure 2, and showed it to have similar, negligible effects on promoter activity in the Aft1-deficient strain (Fig. 3) as seen following cisplatin treatment.

It is possible that cisplatin activation of Aft1 utilizes similar mechanisms to those of iron chelating agents

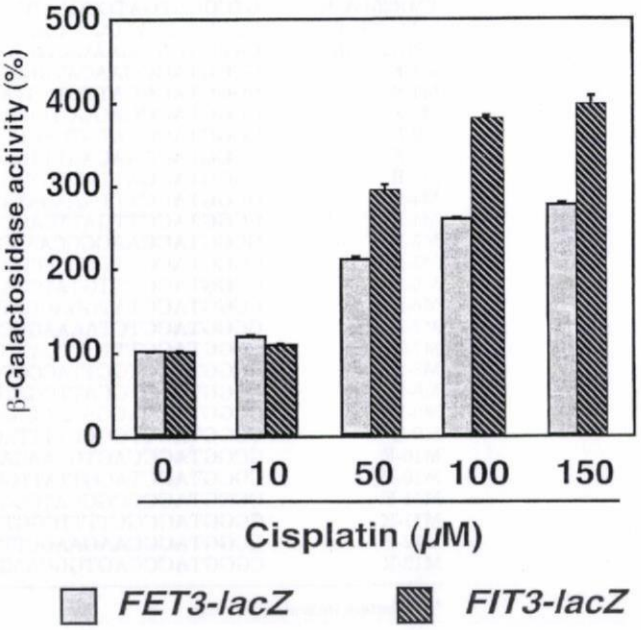

Fig. 1. *FET3* and *FIT3* promoter activation by cisplatin. Wild-type (WT) cells (BY4742) were transformed with either the *FET3-LacZ* or *FIT3-LacZ* construct. The transformed cells were incubated with 0, 10, 50, 100, or 150 μM cisplatin for 3 h and the specific activity of β-galactosidase was measured. Data are mean ± standard deviation (SD) from three independent experiments. β-galactosidase activity of a *FET3-lacZ* or *FIT3-lacZ* control is relatively indicated as 100%.

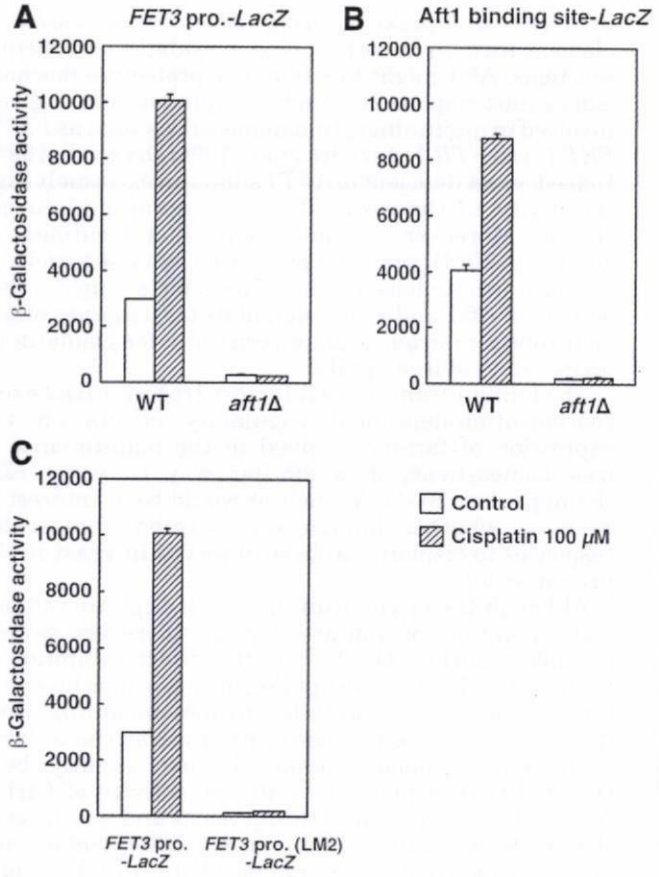

Fig. 2. Aft1 is necessary for cisplatin activation of the *FET3* promoter. WT cells (BY4742) were transformed with the *FET3-LacZ* (**A**), mutant *FET3-LacZ* (LM2) (**B**), or AFT1 binding site-*LacZ* (**C**) construct. The transformed cells were incubated with 0 or 100 μM cisplatin for 3 h and the specific activity of β-galactosidase was measured. Data are mean ± SD from three independent experiments.

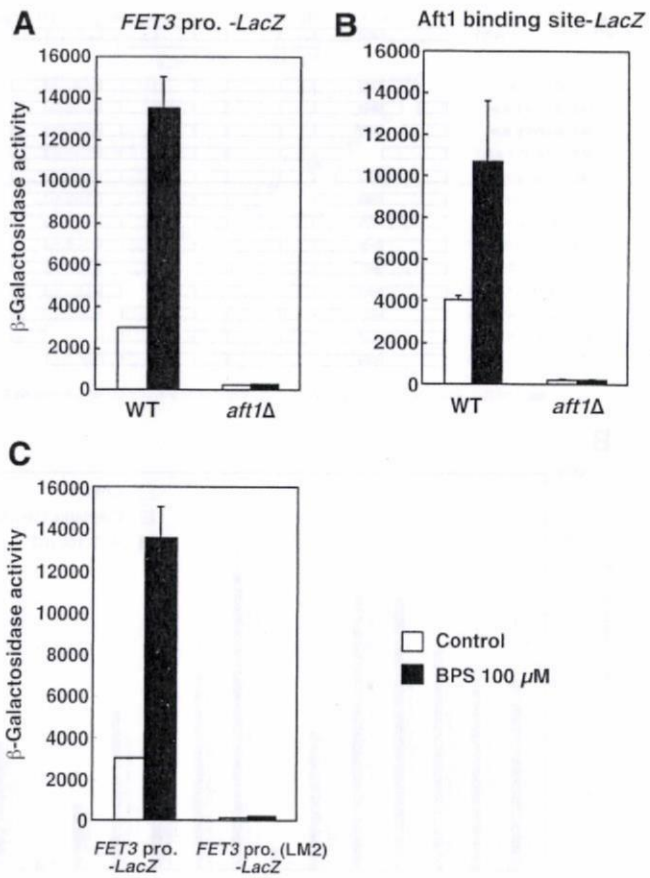

Fig. 3. Aft1 mediates BPS activation of the *FET3* promoter. WT cells (BY4742) were transformed with the *FET3-LacZ* (**A**), mutant *FET3-LacZ* (LM2) (**B**), or AFT1 binding site-*LacZ* (**C**) construct. The transformed cells were incubated with 0 or 100 μM BPS for 3 h and the specific activity of β-galactosidase was measured. Data are mean ± SD from three independent experiments.

that activate Aft1. We therefore examined Aft1 domains involved in activation by cisplatin and BPS and compared the effects of these compounds on Aft1 deletion mutants (Fig. 4A) expressed in Aft1-deleted yeast. The response of the Aft1 deletion mutants M1–M13 to both cisplatin and BPS was found to conform to a similar pattern. The *FET3* promoter could not be activated in yeasts expressing M4 (Δ97–107 a.a.), M7 (Δ271–331 a.a.), or M12 (Δ413–571 a.a.), but activation was observed following treatment with both compounds in yeasts expressing other mutants (Fig. 4B). M4 is a deletion mutant lacking the nuclear export signal (NES) (Yamaguchi-Iwai et al., 2002), while the cysteine (Cys 290) responsible for extra-nuclear transport of Aft1 is located within the domain deleted in M7 (Yamaguchi-Iwai et al., 1995). Both mutants are therefore constitutively present within the nucleus, irrespective of cisplatin or BPS treatment and, as such, are thought to be in a state of permanent transcription activation (Yamaguchi-Iwai et al., 2002). It is likely that activation of the *FET3* promoter in the M12 mutant was not observed following cisplatin and BPS treatment because of the deletion of the transcription domain (Yamaguchi-Iwai et al., 2002). These results indicate that one or more of the three Aft1 domains mutated in M4, M7, and M12 are responsible for activation of the *FET3* promoter by both cisplatin and BPS. Aft1 deletion mutants lacking the amino acids 108–157 and 208–270 were also constructed, but expression of mutated Aft1 was not observed in these yeasts under the conditions of the present study (data not shown). It is important to note that the above findings do not exclude the possibility that cisplatin augments *AFT1* transcription using mechanisms similar to those utilized by BPS.

As we believe that BPS activates Aft1 by inhibiting cellular uptake of iron, the effect of cisplatin on the uptake of $^{55}Fe(II)$ into yeast cells was examined. As shown in Figure 5, cisplatin inhibited iron uptake in a concentration-dependent manner. It is therefore reasonable to assume that cisplatin inhibition of iron uptake leads to activation of Aft1 and the subsequent induction of target genes involved in the maintenance of iron homeostasis.

DISCUSSION

The present study determined that expression of 16 yeast genes is accelerated by cisplatin. Among these are 14 genes that encode proteins involved in the maintenance of iron homeostasis (Table 2) and which are regulated by the transcription factor Aft1 (Yamaguchi-Iwai et al., 1995, 1996) that is activated by a decrease in intracellular iron concentrations (Yamaguchi-Iwai et al., 1995, 2002).

This study is the first to demonstrate the inhibition of cellular iron uptake by cisplatin. When cells are cultured

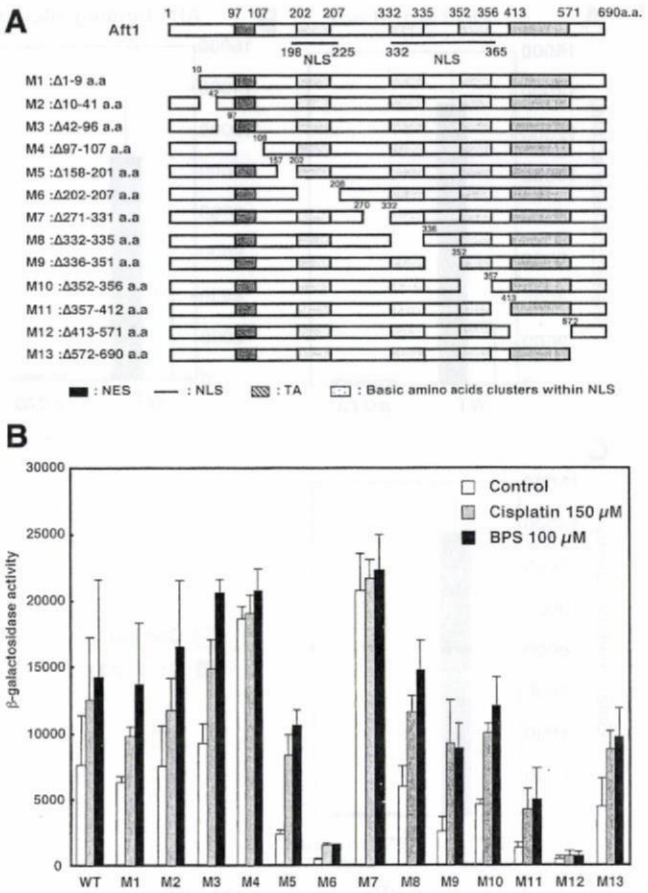

Fig. 4. Analysis of Aft1 domain requirements for cisplatin activation of the *FET3* promoter. **A**: Schematic representation of Aft1 structural domains and deletion mutants. **B**: Aft1 deletion mutants (M1–13) were introduced into WT cells carrying *FET3-LacZ*. Cells were then incubated with 150 μM cisplatin, 100 μM BPS or with no addition (control) and the specific activity of β-galactosidase was measured. Data are mean ± SD from three independent experiments.

in the presence of cisplatin, iron uptake is decreased and the expression of Aft1 target genes is activated. The toxic effects of cisplatin might be induced through its inhibition of uptake of iron, which is an essential element with an important role in oxidation–reduction reactions. Aft1 might function as a protective mechanism against cisplatin through its upregulation of genes involved in maintaining iron homeostasis such as *FET3, FET 4*, and *FTR 1* (Askwith et al., 1994; Dix et al., 1994). Indeed, yeast deficient in *AFT1* shows an extremely high sensitivity to the toxic effects of cisplatin (data not shown). Moreover, we have found that treatment of yeast with Fe(II) provided protection against toxicity of cisplatin (unpublished data). These facts suggest that activity of Aft1 and expression of its target genes might be involved in acquisition of resistance for cisplatin by acceleration of iron uptake.

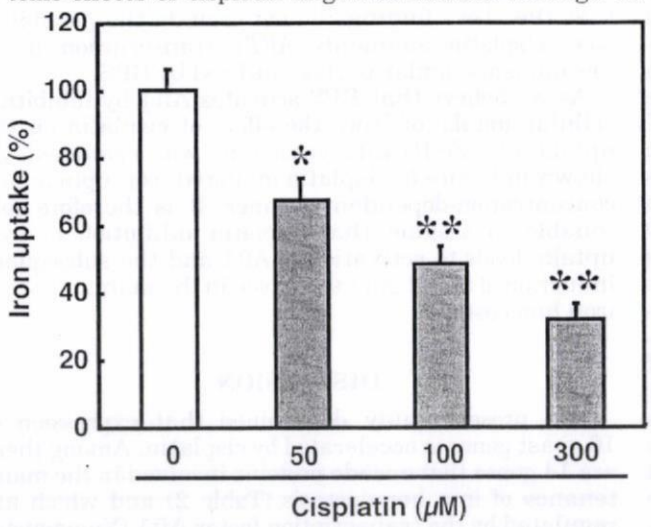

Fig. 5. Effect of cisplatin treatment on iron uptake. WT cells (BY4742) were incubated in assay buffer containing 1 mM $^{55}FeCl_3$ and ascorbate with 0, 50, 100, or 300 μM cisplatin for 2 h. Iron uptake by the cells was measured as described in the Materials and Method. *,**Significantly different from the control ($^{*}P < 0.005$, $^{**}P < 0.001$, Student's *t*-test).

The human transcription factors Irp1 and Irp2 exert concentration-dependent regulatory effects on the expression of factors involved in the maintenance of iron homeostasis, in a similar way to yeast Aft1 (Pantopoulos, 2004). As such, it would be of interest to examine whether human cells exhibit comparable responses to cisplatin to those observed in yeast in the present study.

Although the mechanisms by which cisplatin inhibits cellular uptake of iron are unclear, there are several possible theories. The first is the direct inhibition of proteins involved in iron uptake, as cisplatin is known to bind to various intracellular factors including DNA (Bose, 2002). A second possibility involves the indirect inhibition of copper uptake. It has recently been reported that cisplatin inhibits the activity of Ctrl, a transporter of copper in budding yeasts and human cells (Ishida et al., 2002; Holzer et al., 2004; Safaei and Howell, 2005). The copper oxidase Fet3, which forms a complex with Ftr 1 and is required for iron uptake in yeast, cannot maintain its activity in the absence of copper (De Freitas et al., 2003). It is conceivable that cisplatin inhibition of copper uptake leads to Fet3 inhibition and a subsequent decrease in the amount of iron taken up via the Fet3–Ftr l complex. However, as an alternative study reports that cisplatin does not influence intracellular copper levels in yeasts (Ohashi et al., 2003), further investigation is required into the effects of cisplatin on cellular copper uptake.

Previous microarray studies have been carried out into the effects of cisplatin on the expression of genes in budding yeasts (Birrell et al., 2002; Gatti et al., 2004). Interestingly, these studies did not find any effect on genes involved in the maintenance of iron homeostasis. Earlier investigators cultured yeast on YPAD medium, which is rich in nutrients, while in the present study, we used the synthetic minimum medium, SD medium. The iron concentration of the YPAD medium is higher than the SD medium, so it is possible that cellular concentration of iron did not decrease sufficiently to activate Aft1 in yeasts cultured in YPAD medium, even when iron uptake was inhibited by cisplatin. As an extension of this hypothesis, we speculate that the iron concentration of serum might influence the anticancer effects of cisplatin when used in chemotherapy for the treatment of cancers.

ACKNOWLEDGMENTS

The authors thank Nippon Kayaku Co., Ltd. (Tokyo, Japan) for providing the cisplatin used in this study.

LITERATURE CITED

Aebi S, Kurdi-Haidar B, Gordon R, Cenni B, Zheng H, Fink D, Christen RD, Boland CR, Koi M, Fishel R, Howell SB. 1996. Loss of DNA mismatch repair in acquired resistance to cisplatin. Cancer Res 56:3087–3090.

Alcain FJ, Low H, Crane FL. 1994. Iron reverses impermeable chelator inhibition of DNA synthesis in CCl 39 cells. Proc Natl Acad Sci USA 91:7903–7906.
Askwith C, Eide D, Van Ho A, Bernard PS, Li L, Davis-Kaplan S, Sipe DM, Kaplan J. 1994. The FET3 gene of S. cerevisiae encodes a multicopper oxidase required for ferrous iron uptake. Cell 76:403–410.
Auclair K, Huang HW, Moenne-Loccoz P, Ortiz de Montellano PR. 2003. Cloning and expression of a heme binding protein from the genome of Saccharomyces cerevisiae. Protein Expr Purif 28:340–349.
Birrell GW, Brown JA, Wu HI, Giaever G, Chu AM, Davis RW, Brown JM. 2002. Transcriptional response of Saccharomyces cerevisiae to DNA-damaging agents does not identify the genes that protect against these agents. Proc Natl Acad Sci USA 99:8778–8783.
Bose RN. 2002. Biomolecular targets for platinum antitumor drugs. Mini Rev Med Chem 2:103–111.
Brown SJ, Kellett PJ, Lippard SJ. 1993. Ixr1, a yeast protein that binds to platinated DNA and confers sensitivity to cisplatin. Science 261:603–605.
Dancis A, Klausner RD, Hinnebusch AG, Barriocanal JG. 1990. Genetic evidence that ferric reductase is required for iron uptake in Saccharomyces cerevisiae. Mol Cell Biol 10:2294–2301.
De Freitas J, Wintz H, Kim JH, Poynton H, Fox T, Vulpe C. 2003. Yeast, a model organism for iron and copper metabolism studies. Biometals 16:185–197.
Dix DR, Bridgham JT, Broderius MA, Byersdorfer CA, Eide DJ. 1994. The FET4 gene encodes the low affinity Fe(II) transport protein of Saccharomyces cerevisiae. J Biol Chem 269:26092–26099.
Einhorn LH, Williams SD. 1979. The role of cis-platinum in solid-tumor therapy. N Engl J Med 300:289–291.
Fink D, Zheng H, Nebel S, Norris PS, Aebi S, Lin TP, Nehme A, Christen RD, Haas M, MacLeod CL, Howell SB. 1997. In vitro and in vivo resistance to cisplatin in cells that have lost DNA mismatch repair. Cancer Res 57:1841–1845.
Fox ME, Feldman BJ, Chu G. 1994. A novel role for DNA photolyase: Binding to DNA damaged by drugs is associated with enhanced cytotoxicity in Saccharomyces cerevisiae. Mol Cell Biol 14:8071–8077.
Fu D, Beeler TJ, Dunn TM. 1995. Sequence, mapping and disruption of CCC2, a gene that cross-complements the Ca(2+)-sensitive phenotype of csg1 mutants and encodes a P-type ATPase belonging to the Cu(2+)-ATPase subfamily. Yeast 11:283–292.
Fujii R, Mutoh M, Niwa K, Yamada K, Aikou T, Nakagawa M, Kuwano M, Akiyama S. 1994. Active efflux system for cisplatin in cisplatin-resistant human KB cells. Jpn J Cancer Res 85:426–433.
Furuchi T, Ishikawa H, Miura N, Ishizuka M, Kajiya K, Kuge S, Naganuma A. 2001. Two nuclear proteins, Cin5 and Ydr259c, that confer resistance to cisplatin in *Saccharomyces cerevisiae*. Mol Pharmacol 59:470–474.
Furuchi T, Hwang GW, Naganuma A. 2002. Overexpression of the ubiquitin-conjugating enzyme Cdc34 confers resistance to methylmercury in Saccharomyces cerevisiae. Mol Pharmacol 61:738–741.
Gately DP, Howell SB. 1993. Cellular accumulation of the anticancer agent cisplatin: A review. Br J Cancer 67:1171–1176.
Gatti L, Chen D, Beretta GL, Rustici G, Carenini N, Corna E, Colangelo D, Zunino F, Bahler J, Perego P. 2004. Global gene expression of fission yeast in response to cisplatin. Cell Mol Life Sci 61:2253–2263.
Georgatsou E, Alexandraki D. 1994. Two distinctly regulated genes are required for ferric reduction, the first step of iron uptake in Saccharomyces cerevisiae. Mol Cell Biol 14:3065–3073.
Godwin AK, Meister A, O'Dwyer PJ, Huang CS, Hamilton TC, Anderson ME. 1992. High resistance to cisplatin in human ovarian cancer cell lines is associated with marked increase of glutathione synthesis. Proc Natl Acad Sci USA 89:3070–3074.
Heymann P, Ernst JF, Winkelmann G. 1999. Identification of a fungal triacetylfusarinine C siderophore transport gene (TAF1) in Saccharomyces cerevisiae as a member of the major facilitator superfamily. Biometals 12:301–306.
Heymann P, Ernst JF, Winkelmann G. 2000. Identification and substrate specificity of a ferrichrome-type siderophore transporter (Arn1p) in Saccharomyces cerevisiae. FEMS Microbiol Lett 186:221–227.
Holzer AK, Samimi G, Katano K, Naerdemann W, Lin X, Safaei R, Howell SB. 2004. The copper influx transporter human copper transport protein 1 regulates the uptake of cisplatin in human ovarian carcinoma cells. Mol Pharmacol 66:817–823.
Huang RY, Eddy M, Vujcic M, Kowalski D. 2005. Genome-wide screen identifies genes whose inactivation confer resistance to cisplatin in Saccharomyces cerevisiae. Cancer Res 65:5890–5897.
Ikeda K, Miura K, Himeno S, Imura N, Naganuma A. 2001. Glutathione content is correlated with the sensitivity of lines of PC12 cells to cisplatin without a corresponding change in the accumulation of platinum. Mol Cell Biochem 219:51–56.
Ishida S, Lee J, Thiele DJ, Herskowitz I. 2002. Uptake of the anticancer drug cisplatin mediated by the copper transporter Ctr1 in yeast and mammals. Proc Natl Acad Sci USA 99:14298–14302.
Ishikawa T, Ali-Osman F. 1993. Glutathione-associated cis-diamminedichloroplatinum(II) metabolism and ATP-dependent efflux from leukemia cells. Molecular characterization of glutathione-platinum complex and its biological significance. J Biol Chem 268:20116–20125.
Isoyama T, Murayama A, Nomoto A, Kuge S. 2001. Nuclear import of the yeast AP-1-like transcription factor Yap1p is mediated by transport receptor Pse1p, and this import step is not affected by oxidative stress. J Biol Chem 276:21863–21869.
Kelley SL, Basu A, Teicher BA, Hacker MP, Hamer DH, Lazo JS. 1988. Overexpression of metallothionein confers resistance to anticancer drugs. Science 241:1813–1815.
Kikuchi Y, Iwano I, Miyauchi M, Kita T, Sugita M, Tenjin Y, Nagata I. 1990. Possible mechanisms of resistance to cis-diamminedichloroplatinum (II) of human ovarian cancer cells. Jpn J Cancer Res 81:701–706.
Lesuisse E, Simon-Casteras M, Labbe P. 1998. Siderophore-mediated iron uptake in Saccharomyces cerevisiae: The SIT1 gene encodes a ferrioxamine B permease that belongs to the major facilitator superfamily. Microbiology 144:3455–3462.
Martins LJ, Jensen LT, Simon JR, Keller GL, Winge DR. 1998. Metalloregulation of FRE1 and FRE2 homologs in Saccharomyces cerevisiae. J Biol Chem 273:23716–23721.
Mistry P, Loh SY, Kelland LR, Harrap KR. 1993. Effect of buthionine sulfoximine on PtII and PtIV drug accumulation and the formation of glutathione conjugates in human ovarian-carcinoma cell lines. Int J Cancer 55:848–856.
Naganuma A, Satoh M, Imura N. 1987. Prevention of lethal and renal toxicity of cis-diamminedichloroplatinum(II) by induction of metallothionein synthesis without compromising its antitumor activity in mice. Cancer Res 47:983–987.
Naganuma A, Miura N, Kaneko S, Mishina T, Hosoya S, Miyairi S, Furuchi T, Kuge S. 2000. GFAT as a target molecule of methylmercury toxicity in Saccharomyces cerevisiae. FASEB J 14:968–972.
Niedner H, Christen R, Lin X, Kondo A, Howell SB. 2001. Identification of genes that mediate sensitivity to cisplatin. Mol Pharmacol 60:1153–1160.
Ohashi K, Kajiya K, Inaba S, Hasegawa T, Seko Y, Furuchi T, Naganuma A. 2003. Copper (II) protects yeast against toxicity of cisplatin independently of induction of metallothionein and inhibition of platinum uptake. Biochem Biophys Res Commun 310:148–152.
Pantopoulos K. 2004. Iron metabolism and the IRE/IRP regulatory system: An update. Ann N Y Acad Sci 1012:1–13.
Protchenko O, Ferea T, Rashford J, Tiedeman J, Brown PO, Botstein D, Philpott CC. 2001. Three cell wall mannoproteins facilitate the uptake of iron in Saccharomyces cerevisiae. J Biol Chem 276:49244–49250.
Puig S, Askeland E, Thiele DJ. 2005. Coordinated remodeling of cellular metabolism during iron deficiency through targeted mRNA degradation. Cell 120:99–110.
Safaei R, Howell SB. 2005. Copper transporters regulate the cellular pharmacology and sensitivity to Pt drugs. Crit Rev Oncol Hematol 53:13–23.
Schenk PW, Boersma AW, Brandsma JA, den Dulk H, Burger H, Stoter G, Brouwer J, Nooter K. 2001. SKY1 is involved in cisplatin-induced cell kill in Saccharomyces cerevisiae, and inactivation of its human homologue, SRPK1, induces cisplatin resistance in a human ovarian carcinoma cell line. Cancer Res 61:6982–6986.
Schenk PW, Brok M, Boersma AW, Brandsma JA, Den Dulk H, Burger H, Stoter G, Brouwer J, Nooter K. 2003. Anticancer drug resistance induced by disruption of the Saccharomyces cerevisiae NPR2 gene: A novel component involved in cisplatin- and doxorubicin-provoked cell kill. Mol Pharmacol 64:259–268.
Siddik ZH. 2003. Cisplatin: Mode of cytotoxic action and molecular basis of resistance. Oncogene 22:7265–7279.
Stearman R, Yuan DS, Yamaguchi-Iwai Y, Klausner RD, Dancis A. 1996. A permease-oxidase complex involved in high-affinity iron uptake in yeast. Science 271:1552–1557.
Yamaguchi-Iwai Y, Dancis A, Klausner RD. 1995. AFT1: A mediator of iron regulated transcriptional control in Saccharomyces cerevisiae. EMBO J 14:1231–1239.
Yamaguchi-Iwai Y, Stearman R, Dancis A, Klausner RD. 1996. Iron-regulated DNA binding by the AFT1 protein controls the iron regulon in yeast. EMBO J 15:3377–3384.
Yamaguchi-Iwai Y, Ueta R, Fukunaka A, Sasaki R. 2002. Subcellular localization of Aft1 transcription factor responds to iron status in Saccharomyces cerevisiae. J Biol Chem 277:18914–18918.

Available online at www.sciencedirect.com
ScienceDirect
Toxicology 229 (2007) 33–41
TOXICOLOGY
www.elsevier.com/locate/toxicol

Metallothionein proteins expression, copper and zinc concentrations, and lipid peroxidation level in a rodent model for amyotrophic lateral sclerosis

Eiichi Tokuda [a], Shin-Ichi Ono [a,b,*], Kumiko Ishige [c], Akira Naganuma [d], Yoshihisa Ito [c], Takashi Suzuki [a,e]

[a] *Laboratory of Clinical Pharmacy, College of Pharmacy, Nihon University, Chiba, Japan*
[b] *Division of Neurology, Akiru Municipal Medical Center, Tokyo, Japan*
[c] *Laboratory of Pharmacology, College of Pharmacy, Nihon University, Chiba, Japan*
[d] *Laboratory of Molecular and Biochemical Toxicology, Graduate School of Pharmaceutical Sciences, Tohoku University, Sendai, Japan*
[e] *Department of Pediatrics, Nihon University School of Medicine, Tokyo, Japan*

Received 12 July 2006; received in revised form 6 September 2006; accepted 24 September 2006
Available online 29 September 2006

Abstract

It has been hypothesized that copper-mediated oxidative stress contributes to the pathogenesis of familial amyotrophic lateral sclerosis (ALS), a fatal motor neuron disease in humans. To verify this hypothesis, we examined the copper and zinc concentrations and the amounts of lipid peroxides, together with that of the expression of metallothionein (MT) isoforms in a mouse model [superoxide dismutase1 transgenic (SOD1 Tg) mouse] of ALS. The expression of MT-I and MT-II (MT-I/II) isoforms were measured together with Western blotting, copper level, and lipid peroxides amounts increased in an age-dependent manner in the spinal cord, the region responsible for motor paralysis. A significant increase was already seen as early as 8-week-old SOD1 Tg mice, at which time the mice had not yet exhibited motor paralysis, and showed a further increase at 16 weeks of age, when paralysis was evident. Inversely, the spinal zinc level had significantly decreased at both 8 and 16 weeks of age. The third isoform, the MT-III level, remained at the same level as an 8-week-old wild-type mouse, finally increasing to a significant level at 16 weeks of age. It has been believed that a mutant SOD1 protein, encoded by a mutant *SOD1*, gains a novel cytotoxic function while maintaining its original enzymatic activity, and causes motor neuron death (gain-of-toxic function). Copper-mediated oxidative stress seems to be a probable underlying pathogenesis of gain-of-toxic function. Taking the above current concepts and the classic functions of MT into account, MTs could have a disease modifying property: the MT-I/II isoform for attenuating the gain-of-toxic function at the early stage of the disease, and the MT-III isoform at an advanced stage.

Keywords: Metallothionein; Copper; Zinc; Oxidative stress; Amyotrophic lateral sclerosis; Superoxide dismutase1

1. Introduction

Metallothionein (MT) is a family of low-molecular-weight, cystein-rich, heat-stable and metal binding proteins (Kägi and Schäffer, 1988). MT participates in a broad range of physiological functions such as detoxifi-

* Corresponding author at: Laboratory of Clinical Pharmacy, College of Pharmacy, Nihon University, 7-7-1 Narashino-dai, Funabashi, Chiba 274-8555, Japan. Tel.: +81 47 465 2397; fax: +81 47 465 2397.
E-mail address: shin-ono@pha.nihon-u.ac.jp (S.-I. Ono).

0300-483X/$ – see front matter © 2006 Elsevier Ireland Ltd. All rights reserved.
doi:10.1016/j.tox.2006.09.011

cation of heavy metals like mercury (Hg) and cadmium (Cd), homeostasis of essential metals including copper (Cu) and zinc (Zn), and scavenging reactive oxygen species (ROS) (Aschner et al., 1997; Hidalgo et al., 2001). Four isoforms are identified in mammals, three of which, MT-I, MT-II and MT-III are found in the central nervous system (CNS) (Aschner et al., 1997; Palmiter et al., 1992; Uchida et al., 1991). The localization and induction patterns between the MT-I and MT-II (MT-I/II) isoforms and the MT-III isoform in the CNS appear to be distinct. The expression of MT-I/II is mainly localized in glias (Aschner et al., 1997; Blaauwgeers et al., 1993) and is induced by exposure to metals including Hg, Cd, Cu and Zn, cytokines and ROS (Aschner et al., 1997; Hidalgo et al., 2001). On the other hand, the MT-III isoform is mainly present in neurons (Masters et al., 1994; Uchida et al., 1991), and is not easily induced by exposure to the above agents (Zheng et al., 1995).

Amyotrophic lateral sclerosis (ALS) is a lethal motor neuron disease characterized by selective degeneration of motoneurons, resulting in muscular atrophy including respiratory and bulbar muscles, complete paralysis, and death (Rowland and Shneider, 2001). Approximately 90% of ALS is sporadic and the remaining 10% or so is familial (Cleveland and Rothstein, 2001). Rosen et al. found that about 20% of familial ALS is linked with mutations of the gene encoding Cu/Zn superoxide dismutase (*SOD1*) (Rosen et al., 1993). It has been believed that abnormal SOD1 proteins encoded by mutant *SOD1* do not lose their original enzymatic function but gain a novel cytotoxic function in motoneurons (gain-of-toxic function theory) (Bruijn et al., 2004; Gurney et al., 1994). A presumable mechanism of the gain-of-toxic function is a Cu-mediated oxidative stress. A point mutation in *SOD1* causes chemical structure changes of SOD1 proteins (misfolding proteins), while retaining its original activity and with subsequent clumsy handling of Cu and Zn (Beckman et al., 2001; Bruijn et al., 2004; Valentine and Hart, 2003). As a result of decreased Zn-binding affinity and higher affinity for Cu (Crow et al., 1997; Lyons et al., 1996), Cu-mediated oxidative stress is enhanced, and leads to neuronal death (Said Ahmed et al., 2000; Wiedau-Pazos et al., 1996).

Mouse carrying a human mutant *SOD1* develops an ALS-like disease, and is a good animal model for ALS research. The mice do no exhibit any clinical signs of motor paralysis up to the age of about 12 weeks, and develop paralysis at the age of 14–16 weeks, dying of respiratory failure by 17–18 weeks old (Bruijn et al., 1997; Gurney et al., 1994; Ripps et al., 1995).

In this way, all physiological functions of MT are likely to be associated with the presumable current pathogenesis of ALS. In order to investigate the possible role of the changes in Cu and Zn concentrations and lipid peroxides (LPO) products, we therefore measured temporal changes in the Cu and Zn levels and the amount of LPO together with MT-I/II and MT-III proteins in a rodent model for ALS.

2. Materials and methods

2.1. Chemicals

An enhanced chemiluminescence (ECL) agent, glutathione-sepharose 4B and polyvinylidene difluoride (PVDF) membranes were purchased from Amersham Bioscience (Buckinghamshire, UK). The Protein Assay Rapid Kit$_{WAKO}$ and reduced glutathione buffer were obtained from Wako Pure Chemical Industries Ltd. (Osaka, Japan). The pGEM-T Easy vector systems were purchased from Promega K.K. (Tokyo, Japan). Mouse monoclonal anti MT-I/II antibody (clone: E9) was purchased from Dako Cytomation Inc. (Carpinteria, CA, USA). Recombinant MT-I and MT-II proteins, mouse monoclonal anti β-tubulin (clone: TUB 2.1) and mouse monoclonal horseradish conjugated anti IgG antibody were from Sigma Chemical Co. (St. Louis, MO, USA).

2.2. Animals

We used G93A SOD1 transgenic (SOD1 Tg) mice [B6SJL-Tg (SOD1-G93A)^{dl} 1 Gur/J; 002300] as a model for familial ALS (Gurney et al., 1994). The mice were purchased from The Jackson Laboratory (Bar Harbor, ME, USA) and were housed under standard conditions (temperature 22 °C, relative humidity 60%, 12 h light/dark cycle, and free access to food and water) in the animal facility at the College of Pharmacy, Nihon University. The SOD1 Tg male mice were crossed with CF-1 wild-type (WT) female mice. When they were at the age of 8 or 16 weeks, three to five each of male SOD1 Tg and WT mice were killed by decapitation under light anesthesia. The spinal cord (the region responsible for paralysis) and the cerebellum [non-responsible (control) region] were immediately dissected on a glass plate on crushed ice, were frozen in liquid nitrogen, then stored at −80 °C until use. The present study was approved by the ethics committee for laboratory animal use at the College of Pharmacy, Nihon University.

2.3. Motor function testing (infrared beam test)

The motor performance was assessed by the infrared beam test with Digiscan (Omnitech Electronics Inc., Columbus, OH, USA). Briefly, two sets of infrared beams placed at a distance of 5 cm from the transparent acrylic box floor, traversed the area in perpendicular directions. The beam obstructions served as indicators of the horizontal activities of the mice. An additional set of beams located at a distance of 10 cm from the box floor was used to determine the vertical activities (mice standing on two hind paws). The motor performance was measured weekly

from 4 to 17 weeks of age. The mice were first allowed to acclimatize themselves to the observation situation in a box with infrared sensors prior to the measurements of the motor performance. They were then individually placed in the box, and their motor performance was measured every minute for 5 min. The activity of the mice was expressed as the average count per min (counts/min).

2.4. PCR analysis of the genotype for G93A SOD1 transgenic mice

All offspring were genotyped using the polymerase chain reaction (PCR) process on genomic DNA isolated from their tails, which were digested overnight with proteinase K at 50 °C. The PCR primers to detect mutant *SOD1* transgene were selected according to the recommendations of The Jackson Laboratory: sense, 5′-CAT CAG CCC TAA TCC ATC TGA-3′, and antisense, 5′-CGC GAC TAA CAA TCA AAG TGA-3′. PCR sessions were performed for 30 cycles under the following conditions: denaturation at 94 °C for 1 min, annealing at 55 °C for 45 s and extension at 72 °C for 1 min 20 s. The primers amplified a 236 bp DNA region from mice carrying the human mutant *SOD1* gene (Gong and Elliott, 2000).

2.5. Preparation of the mouse monoclonal antibody specific for MT-III

MT-III cDNA of the entire coding regions was amplified by RT-PCR. The PCR products were ligated into the pGEM-T Easy expression vector as previously described (Hanahan, 1983). MT-III-glutathione-*S*-transferase (MT-III-GST) fusion protein was expressed in *E. coli* and purified on an affinity column with immobilized glutathione-sepharose 4B. BALB/c male mice were immunized with MT-III-GST fusion protein. The fusion protocol, mouse myeloma with immunized mouse spleen cells, was described previously (Köhler and Milstein, 1975). The power and specificity of the antibody were tested using Western blot analysis. The anti MT-III antibody recognized only the recombinant MT-III protein at the expected position (16.8 kDa), but neither the MT-I nor MT-II protein (Fig. 1).

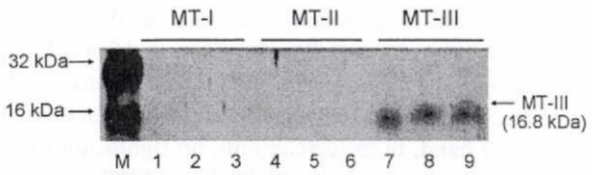

Fig. 1. Specific reactivity of prepared anti metallothionein III antibody. Two micrograms each of metallothionein (MT)-I, MT-II, and MT-III recombinant proteins were electrophoresed on an 18% SDS-polyacrylamide gel, transferred to polyvinylidene difluoride membranes and immunoreacted with the mouse monoclonal anti MT-III antibody. M: molecular marker, MT-I, MT-II and MT-III denote recombinant MT-I, MT-II and MT-III proteins, respectively (three lanes each).

2.6. Protein preparation and iodoacetamide treatment

Spinal cord and cerebellum tissues obtained from both SOD1 Tg and WT mice at 8- and 16-week-old were homogenized in a lysated buffer containing 10 mM Tris–HCl (pH 7), 5 mM EDTA, 1 mM phenylmethylsulfonylfluoride, 137 mM sodium chloride, 1% NP-40 and 10% glycerine. After treatment with sonication for 20 s for three times, the homogenates were centrifuged at 9000 × *g* for 30 min, and the supernatants were saved. The protein extracts were treated with 10% iodoacetamide and 10% tributyl phosphine/isopropanol. The mixtures were incubated in a water bath at 60 °C for 50 min. After cooling on ice, the samples treated with iodoacetamide were centrifuged at 800 × *g* for 5 min, and then the supernatants were collected.

Protein concentration was determined with the pyrogallol red method according to the manufacturer's directions (Protein Assay Rapid Kit_{wako}, Wako Pure Chemicals, Osaka, Japan). Briefly, homogenized samples were mixed with the pyrogallol red-molybdate agent in microplate wells. The mixtures in the wells were left for 20 min at room temperature and then measured by a microplate reader (3550, Bio-Rad, Hercules, CA, USA) furnished with a 600 nm wavelength filter.

2.7. SDS-PAGE and Western blotting

An aliquot of 20 μg protein treated with iodoacetamide was separated on an 18% polyacrylamide gel with Laemmli system (Laemmli, 1970) at 100 V until the tracking dye, containing 10 mM Tris–HCl (pH 7.5), 10 mM EDTA, 20% glycerol, 1% SDS, 0.025% bromophenol blue, 100 mM DTT and 0.7 M 2-mercaptoethanol, reached the bottom of the gel. Electrophoresed proteins were transferred to PVDF membranes at 100 V for 3 h. After transferring, the membranes were blocked in the solutions containing 3% BSA, 1 M Tris–HCl (pH 7.5) and 40 mM sodium chloride for 1 h at room temperature and immunoblotted overnight at 4 °C with the primary antibodies used against mouse monoclonal anti MT-I/II antibody (dilution at 1:100), mouse monoclonal anti MT-III antibody and mouse monoclonal anti β-tubulin (dilution at 1:10,000). After washing with TBS containing 0.1% Tween-20 solution, the membranes were incubated with a mouse monoclonal horseradish conjugated anti IgG antibody (dilution at 1:10,000) for 1 h at room temperature. Immunoreaction was visualized using the ECL agent. After exposure, films were scanned by an image analyzer (LAS1000 plus lumino-image analyzer, Fuji Film, Tokyo, Japan). Band intensities were quantified with NIH images (National Institutes of Health, Bethesda, MD, USA). The expression of MT-I/II or MT-III protein was determined as a ratio of MT-I/II or MT-III to β-tubulin.

2.8. Analysis of copper and zinc concentrations

Spinal cord and cerebellum samples were digested in concentrated nitric acid (65%, v/v) overnight at room temperature

until no visual resides remained. The tissues were incubated in a boiling water bath for 1 h to facilitate digestion. Digested tissues were diluted in ultra-pure water. Copper and zinc concentrations in each sample tissue were measured by inductively coupled plasma mass spectrometry (Agilent 7500, Yokogawa Analytical Systems, Tokyo, Japan). Blanked samples were processed in the same ways. Metal concentrations were reported in micrograms per gram of wet tissue weight.

2.9. Measurement of lipid peroxides

The LPO concentration was determined using the thiobarbituric acid (TBA) method as described elsewhere (Ono et al., 1998). Briefly, tissues were homogenized in ice-cold PBS. All subsequent steps were performed using amber-colored tubes. The homogenized samples were added to 40 mM sulfuric acid and 10% phosphotungstic acid, and then were centrifuged at 1500 × *g* for 10 min. A TBA agent containing 8.8 M acetic acid and 20 mM TBA was added. Samples were incubated in a boiling bath for 1 h. After cooling with tap water for 5 min, *n*-butanol was added in order to extract the malondialdehyde, and the mixture was shaken vigorously by hand. After centrifugation at 1500 × *g* for 10 min, the *n*-butanol phase was saved. The absorbance of the supernatant (*n*-butanol phase) was measured with a spectofluorometer (FP 6200, Nihon Bunko, Tokyo, Japan) at an excitation wavelength of 515 nm and an emission wavelength of 553 nm. The LPO level was estimated using 1,3,3-tetraetoxypropane as a reference standard. Results were expressed as nanomoles of malondialdehyde reactive substances per gram of wet tissue weight.

2.10. Statistical analysis

All the data on the motor performance were represented as mean ± S.E.M. We used repeated-measures ANOVA to compare the motor performance of the SOD1 Tg with that of the WT mice. All other statistical analyses were carried out using Student's *t*-test, including comparison of the values between the SOD1 Tg and WT mice and between the 8- and 16-week-old mice. P values < 0.05 were considered to be statistically significant.

3. Results

3.1. Activity of the G93A SOD1 transgenic mouse

The vertical activities of the mice are shown in Fig. 2. The SOD1 Tg mice showed no signs of paralysis up to the age of 12 weeks, and thereafter began to exhibit a week-dependent decrease in activity, showing the development of motor paralysis. At 16 weeks of age, an evident reduction in vertical activity was observed. The horizontal activities of the mice showed the same pattern (data not shown).

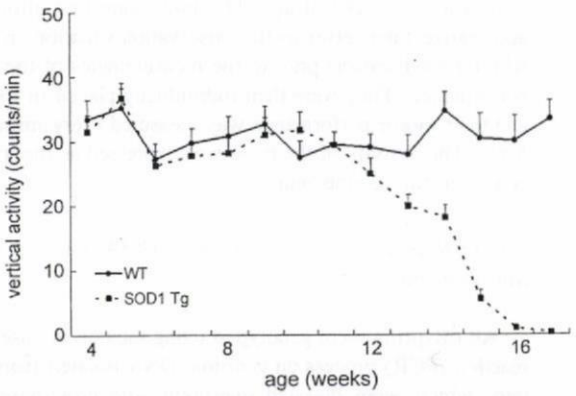

Fig. 2. Time-course of changes in the motor performance in the G93A SOD1 transgenic mice. The motor performance of the mice was measured by the infrared beam test. Significant difference in the vertical activities was found between the G93A SOD1 transgenic (SOD1 Tg) mice and the wild-type (WT) mice ($p = 1.38 \times 10^{-6}$; repeated-measures ANOVA). The motor performance in the SOD1 Tg mice showed a sharp week-dependent decrease after 12 weeks of age, suggestive of development and progression of paralysis ($p = 5.38 \times 10^{-22}$; repeated-measures ANOVA).

3.2. MT-I/II protein expression

The expression of MT-I/II protein in the spinal cord, the region responsible for motor paralysis, is shown in Fig. 3A and B. The protein level had already significantly increased in SOD1 Tg mice at 8 weeks of age, at which time the mice had not yet developed paralysis (Fig. 3A and B). At 16 weeks of age, when paralysis became apparent, the increase in the MT-I/II levels was maintained, with levels significantly higher than that at 8 weeks of age (Fig. 3A and B). On the other hand, the levels of MT-I/II protein in the cerebellum, which is not responsible for paralysis, did not show any differences between SOD1 Tg and WT mice at either 8 or 16 weeks of age (Fig. 3C and D).

3.3. MT-III protein expression

In 8-week-old SOD1 Tg mice, the MT-III levels in the spinal cord remained the same as those of the WT mice (Fig. 4A and B). However, at 16 weeks of age, when SOD Tg mice exhibited motor paresis, the MT-III level had significantly increased (Fig. 4A and B). On the other hand, in the cerebellum, no significant difference was observed between SOD1 Tg and WT mice at either 8 or 16 weeks of age (Fig. 4C and D).

3.4. Copper and zinc concentrations

Cu concentrations in the SOD1 Tg mouse spinal cord showed a significant increase compared with those of

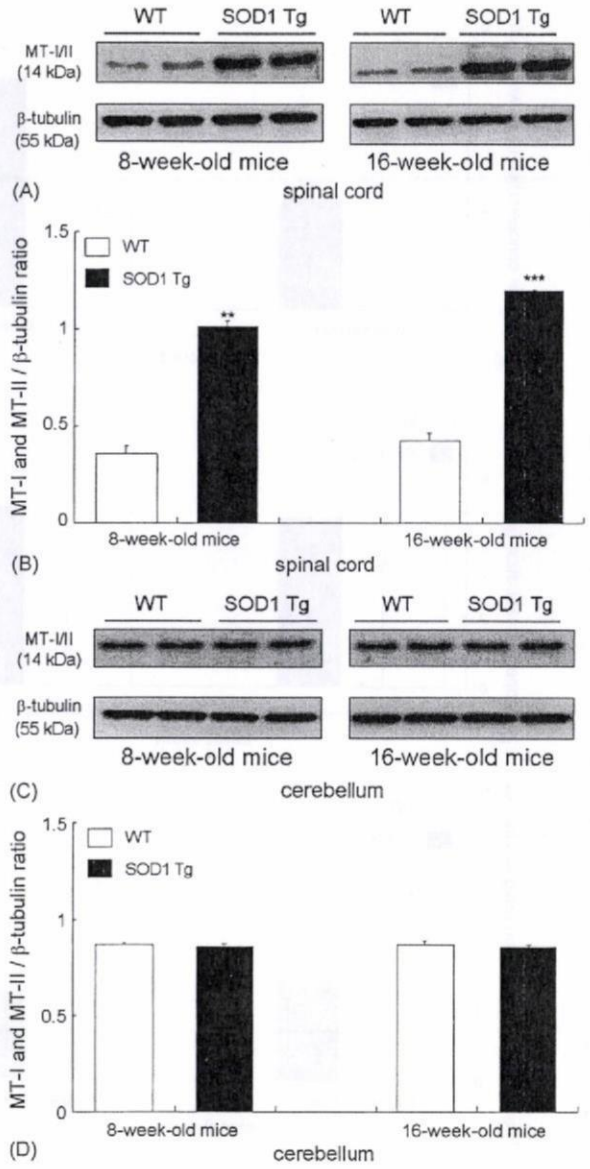

Fig. 3. Changes in metallothionein I and II proteins in G93A SOD1 transgenic mice. The spinal cord is the region responsible for motor paralysis in G93A SOD1 transgenic (SOD1 Tg) mice. Metallothionein-I and II (MT-I/II) proteins were significantly increased in the spinal cord of 8-week-old SOD1 Tg mice [$p = 1.9 \times 10^{-4}$ vs. 8-week-old wild-type (WT) mice], when motor paralysis was not yet apparent. At 16 weeks of age, when the SOD1 Tg mice had developed evident paralysis, MT-I/II proteins showed a further increase ($p = 5.8 \times 10^{-5}$ vs. 8-week-old WT and $p = 0.019$ vs. 8-week-old SOD1 Tg mice) (panels A and B). The cerebellum is not a region responsible for motor paralysis. Cerebellar MT-I/II levels showed no differences between SOD1 Tg and WT mice at either 8 or 16 weeks of age (panels C and D). Data from three to five mice each are shown as mean ± S.E.M. (panels B and D). Western blot analyses from each mouse (SOD1 Tg and WT mice) are shown in panels A and C. $^{**}p < 0.01$; $^{***}p < 0.001$ by Student's *t*-test.

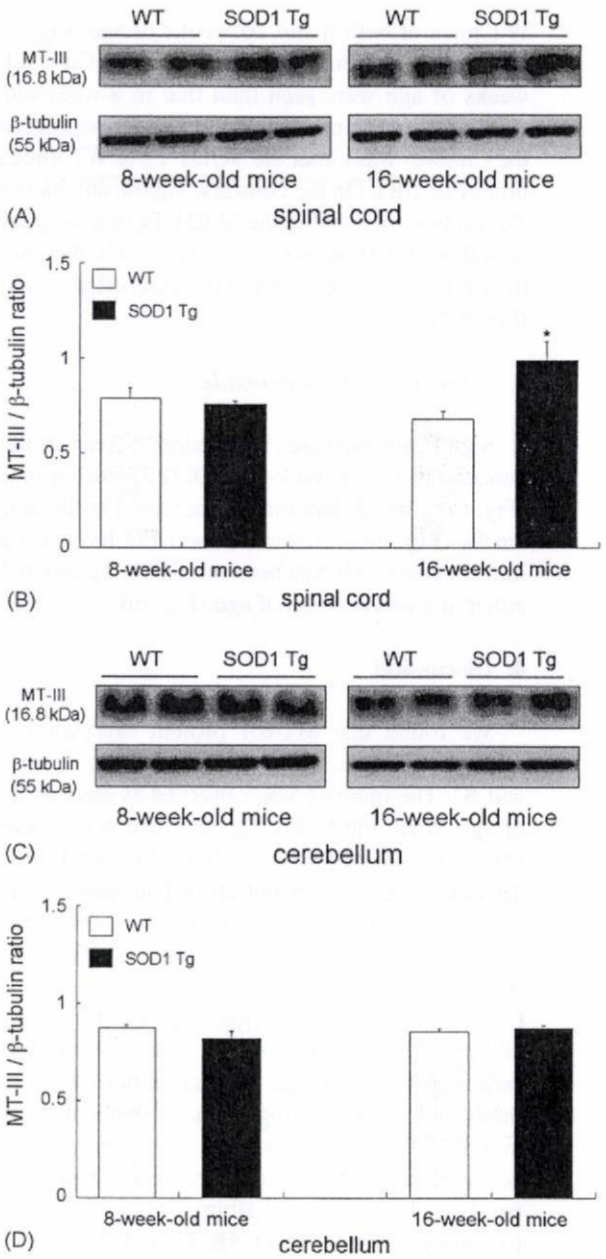

Fig. 4. Changes in metallothionein III protein in G93A SOD1 transgenic mice. In 8-week-old G93A SOD1 transgenic (SOD1 Tg) mice, when the mice were still asymptomatic, no change in MT-III protein level was observed in the spinal cord. However at 16 weeks of age, when SOD1 Tg mice were clearly symptomatic, MT-III level was significantly increased [$p = 0.04$ vs. wild-type (WT) mice at the same age, and $p = 0.02$ vs. 8-week-old SOD1 Tg mice] (panels A and B). No change in MT-III level was observed in the cerebellum at any age (panels C and D). Data from three to five mice each are shown as mean ± S.E.M. (panels B and D). Western blot analyses from each mouse (SOD1 Tg and WT mice) are shown in panels A and C. $^{*}p < 0.05$ by Student's *t*-test.

WT mice at both 8 and 16 weeks of age (Fig. 5A). In SOD1 Tg mice, further increases in the Cu level at 16 weeks of age were seen than that in 8-week-old mice (Fig. 5A). In the cerebellum, however, no alteration in the Cu level was either the SOD1 Tg or WT mice at any time (Fig. 5B). On the contrary, significant decreases in Zn levels were noted in the SOD1 Tg mouse spinal cord at both 8 and 16 weeks of age (Fig. 5C). No change in the Zn level was observed in the cerebellum at any time (Fig. 5D).

3.5. Amounts of lipid peroxides

Significant increases were already seen in the LPO concentration in 8-week-old SOD1 Tg mice spinal cords (Fig. 6A), which had further increased at the age of 16 weeks (Fig. 6A). However, the LPO level in cerebellum showed no change between SOD1 Tg and WT mice either at 8 or 16 weeks of age (Fig. 6B).

4. Discussion

We found that MT-I/II protein expression significantly increased in spinal cord of SOD1 Tg mice (Fig. 3A and B). The increase was observed as early as 8 weeks of age, when the SOD1 Tg mice had not yet exhibited any symptoms of motor paralysis. In 8-week-old SOD1 Tg mice, the Cu concentration had also significantly increased, with an inverse decrease in Zn levels and a concomitant elevation of LPO amounts in the spinal cord (Figs. 5A, C, and 6A). The increase in the MT-I/II and Cu levels increased in an age-dependent manner, being higher at 16 than at 8 weeks of age. Based on these results, we propose that these conditions were strongly implicated in the pathogenesis of motor neuron death in SOD1 Tg mice, since these observations exclusively occurred in the spinal cord, the region responsible for paralysis, but not in cerebellum, a region not responsible for paralysis (Figs. 3C, D, 5B, D, and 6B).

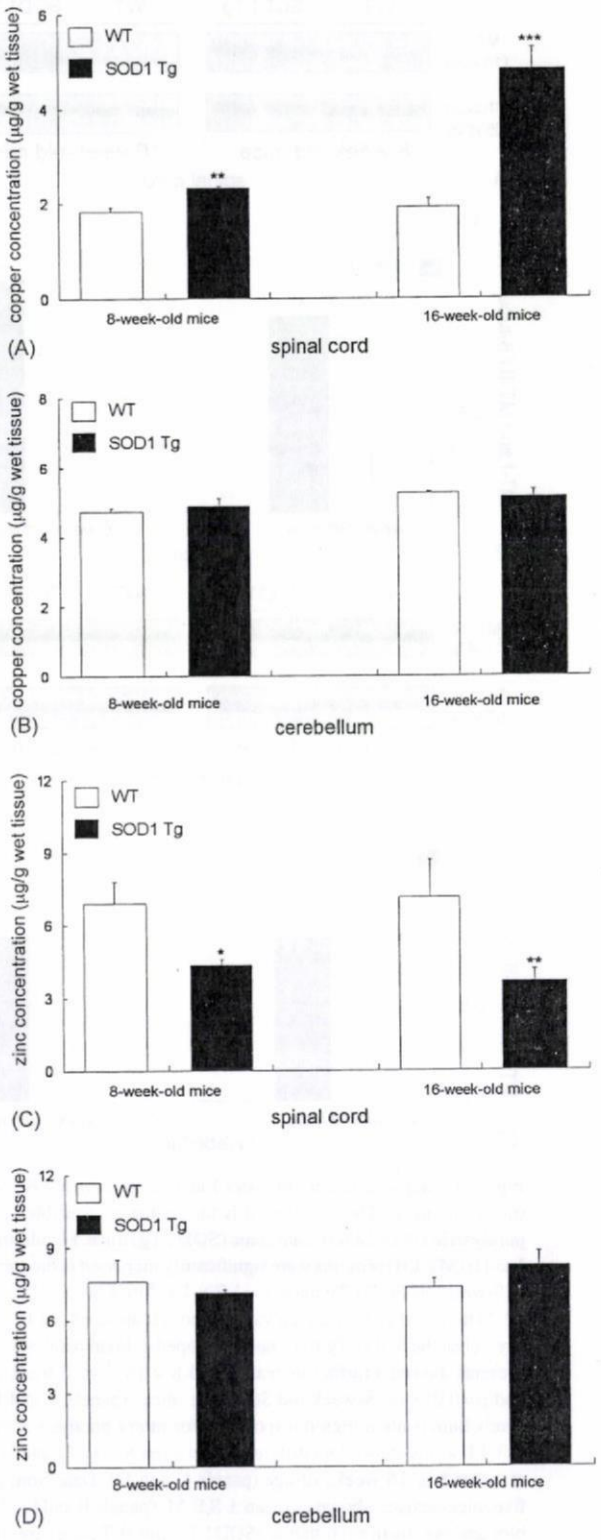

Fig. 5. Copper and zinc concentrations in G93A SOD1 transgenic mice. A significant increase in copper concentration was observed in the spinal cord of the as-yet-asymptomatic 8-week-old G93A SOD1 transgenic (SOD1 Tg) mice [$p = 1.9 \times 10^{-3}$ vs. wild-type (WT) mice at the same age], with a further increase at 16 weeks of age ($p = 3.0 \times 10^{-4}$ vs. WT at the same age, and $p = 6.0 \times 10^{-4}$ vs. 8-week-old SOD1 Tg mice) (panel A). An inverse decrease in zinc level was observed in both 8- and 16-week-old SOD1 Tg mice ($p = 0.02$ vs. 8-week-old WT mice, and $p = 9.2 \times 10^{-4}$ vs. 16-week-old WT (panel C). In the cerebellum, no alternation was found either in copper or zinc level (panels B and D). Data from three to five mice each are shown as mean ± S.E.M. $^{*}p < 0.05$; $^{**}p < 0.01$; $^{***}p < 0.001$ by Student's t-test.

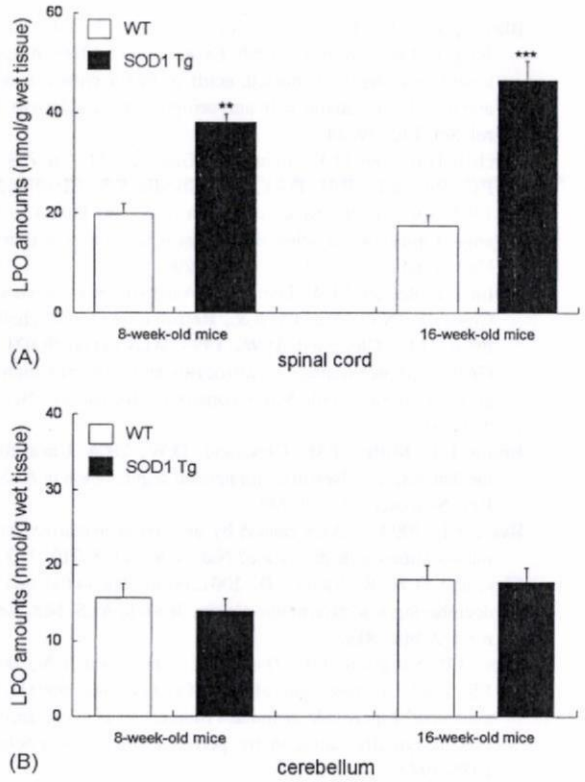

Fig. 6. Lipid peroxides in G93A SOD1 Transgenic mice. Lipid peroxides (LPO) levels were significantly increased in the spinal cord of both 8-week-old G93ASOD1 transgenic (SOD1 Tg) mice and 16-week-old SOD1 Tg mice [$p = 2.0 \times 10^{-3}$ vs. 8-week-old wild-type (WT) mice and $p = 3.1 \times 10^{-5}$ vs.16-week-old WT mice] (panel A). In the cerebellum, no significant change was found in the LPO level at any age (panel B). $^{**}p < 0.01$; $^{***}p < 0.001$ by Student's *t*-test.

The present findings are partially in agreement with previous reports. An increase in the spinal MT-I/II isoform was reported in this line of transgenic mouse (Gong and Elliott, 2000; Nagano et al., 2001; Olsen et al., 2001) or in patients with ALS (Blaauwgeers et al., 1996; Sillevis Smitt et al., 1994). We reported, on the basis of the mRNA findings, that *MT-I* up-regulation was taking place as early as 8 weeks of age in the same line of transgenic mouse spinal cord, but not in the cerebellum (Ono et al., 2006). Although an elevation of Cu concentration was previously reported in the same line of SOD1 Tg mouse (Bush, 2002), no study has previously revealed an increase in Cu and a concomitant inverse decrease in Zn levels in the spinal cord of the same SOD1 Tg mouse at as early as 8 weeks of age.

It is currently accepted that mutant SOD1 is implicated in the pathogenesis of familial ALS. The mutant SOD1 is believed to gain a novel cytotoxic function, while retaining its original enzymatic activity (gain-of-toxic function theory) (Bruijn et al., 2004; Gurney et al., 1994). The mutant SOD1 is characterized by clumsy handling of Cu and Zn (Beckman et al., 2001; Bruijn et al., 2004; Valentine and Hart, 2003), and subsequent alternations in Cu and Zn levels likely play an important role in the gain-of-toxic function (Borchelt et al., 1994). Some evidence exists to support the idea; First, Cu-chelating agents such as D-penicillamine and trientine extend survival in SOD1 Tg mice (Andreassen et al., 2001; Hottinger et al., 1997; Nagano et al., 2003). Second, *atp7b*, encoding Cu-transporting ATPase, is down-regulated in the spinal cord of SOD1 Tg mice (Olsen et al., 2001). Third, crossing an SOD1 Tg mouse with a mouse model for Menkes' disease, which causes congenital Cu deficiency, extend the clinical duration of survival (Kiaei et al., 2004). Fourth, a Zn decrease in mutant SOD1 causes peroxynitrate-mediated tyrosine nitration (Beckman et al., 1993; Estévez et al., 1999) and an increase in biological 3-nitrotyrosin, a hallmark of protein nitration, in the spinal cord in patients with ALS (Beal et al., 1997). Liu et al. demonstrated that ROS production increased with aging, measured by using a spin trap, azulenyl nitrone, in the spinal cord of the SOD1 Tg mouse (Liu et al., 1998). The present study revealed that in 8-week-old SOD1 Tg mice, LPO amounts, measured as malondialdehyde reactive substances, exclusively accumulated in the region responsible for motor paralysis, namely the spinal cord, before the onset of paralysis (Fig. 6A and B). Based on these findings, LPO accumulation is a probable result of Cu and Zn changes in the spinal cord, presumably due to Cu-mediated oxidative stress. Taking the classic functions of the MT-I/II isoform into account, it is reasonable to postulate that the spinal MT-I/II protein increase observed in the present study is a compensatory induction in response to Cu-mediated oxidative stress.

We also found that MT-III protein levels significantly increased in the SOD1 Tg mouse spinal cord (Fig. 4A and B), which was exclusively observed in the paralysis-responsible spinal cord, as was the case with the MT-I/II isoforms. Although *MT-III* mRNA changes have previously been reported (Gong and Elliott, 2000; Olsen et al., 2001), no MT-III protein study has been shown in this line of transgenic mouse. It should be emphasized that unlike MT-I/II, the MT-III protein remained unchanged in 8-week-old SOD1 Tg mice and finally increased at 16 weeks of age, at the end stage of the disease (Fig. 4A and B). The spinal Cu level in 16-week-old SOD1 Tg mice was further increased compared with 8-week-old mice (Fig. 5A), suggesting further LPO production. Nevertheless, the concentration of spinal LPO at 16 weeks of age was not higher than that in 8-week-old mice (Fig. 6A). However, as MT-III protein synthesis induction occurred